Published in the Journal of Heat Transfer for
Fluid Mechanics Institute, June 1951, Stanford University.
Stanford, Cal.

TECHNICAL REPORT NO. 3

RSC

HEAT TRANSFER AND PRESSURE DROP DATA FOR HIGH HEAT FLUX DENSITIES TO WATER AT HIGH SUBCRITICAL PRESSURES

BY

WARREN M. ROHSENOW AND JOHN A. CLARK

FOR

THE OFFICE OF NAVAL RESEARCH
CONTRACT N5ori-07827
NR-035-267
D.I.C. PROJECT NUMBER 6627

APRIL 1, 1951

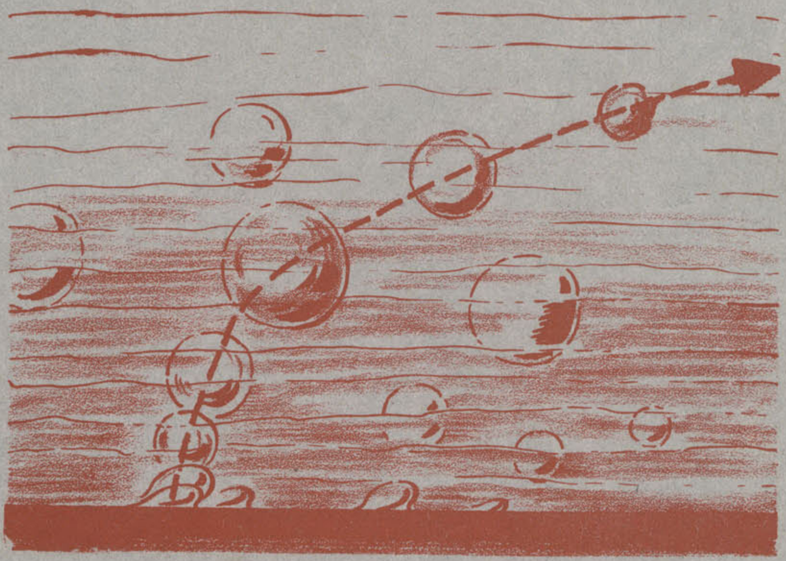

MASSACHUSETTS INSTITUTE OF TECHNOLOGY
DIVISION OF INDUSTRIAL COOPERATION
CAMBRIDGE 39, MASSACHUSETTS

TECHNICAL REPORT NO. 3

HEAT TRANSFER AND PRESSURE DROP DATA FOR HIGH HEAT FLUX DENSITIES TO WATER AT HIGH SUBCRITICAL PRESSURES

by

Warren M. Rohsenow and John A. Clark

For the Office of Naval Research

N5 ori-07827

NR 035-267

DIC PROJECT NO. 6627

April 1, 1951

DIVISION OF INDUSTRIAL COOPERATION

Massachusetts Institute of Technology

Cambridge, Massachusetts

HEAT TRANSFER AND PRESSURE DROP DATA FOR HIGH HEAT FLUX DENSITIES TO WATER AT HIGH SUBCRITICAL PRESSURES

by

Warren M. Rohsenow* and John A. Clark**

SUMMARY

Local surface coefficients of heat transfer, overall pressure drop data and mean friction factor are presented for heat fluxes up to $3.5\text{x}10^6$ Btu/hr ft² for water flowing in a nickel tube under the following conditions: mass rates of flow up to $5.6\text{x}\ 10^6$ lb_m/hr ft² (or inlet velocities up to 30 ft/sec), absolute pressures up to 2000 psia, and liquid subcooling between 50 F and 250 F. The test section dimensions were 0.180 inch I.D. and 9.4 inches long.

INTRODUCTION

Very little information has been available to predict heat transfer and pressure drop performance for liquids with severe temperature gradients adjacent to the surface, particularly when the surface temperature exceeds the normal boiling temperatures. Recent works published by Knowles (3), Kreith and Summerfield (1) (2), and McAdams et al (4) present data for this type heat transfer process in the lower pressure ranges. The data presented here for water was obtained in August, 1950, and represents some of the initial data available for water at pressures up to 2000 psia. Simultaneously, similar data has been gathered at U.C.L.A. This particular type of heat transfer process is encountered in liquid-cooled rocket motors and in more recent steam power plant equipment.

---

* Asst. Prof. Mech. Eng., M. I. T., Cambridge, Mass.

** Instructor, Mech. Eng., M. I. T., Cambridge, Mass.

APPARATUS

The test apparatus is a closed system consisting of a vertical test section of pure nickel, a Hayward-Tyler centrifugal pump, a calibrated orifice, a heat exchanger, a pressure vessel, and an ion exchanger. A layout is given in Fig. 1. Power is supplied from two 36 KW 12 volt DC Generators driven by 440 volt, 3 phase, AC 600 rpm synchronous motors. The generator outputs are connected in series and provide a range of 0-24 volts and 0-3000 amperes. Thermocouples are located at the test water inlet and outlet and along the outer wall of the test section, readings being taken by means of a Rubicon potentiometer, Model 2703 and a Rubicon spotlight galvanometer Model 3401-H. A bourdon type Heise pressure gage 0-2000 psi is located at the inlet to the test section. A Barton differential pressure gage 0-300 inches of water is connected across inlet and outlet of the test section to record the pressure drop.

The test section (figure 2) consists of a pure nickel tube (International Nickel Co. "L" Nickel) of .1805 in. inside diameter, .2101 in. outside diameter, and a length of 9.4 inches. Threaded bushings of "L" nickel are gold soldered to each end of the test section, and make contact with bronze end mounts, which support the test section assembly and carry current from the bussbars.

The test water was circulated by a four-stage centrifugal pump manufactured by Hayward-Tyler Company, Ltd., of England. The pump impeller and the motor assembly are both enclosed in a single stainless steel casing capable of being operated at a pressure of 4000 psia with a head of 300 ft. of water at 50 gpm. The heat exchange system which removes heat equal to the electrical energy supplied employes an intermediate fluid, silicone DC-701, between the test and city cooling water, in order to assure an absence of local boiling of the cooling water in this part of the circuit. Flow measurements were made by a calibrated orifice with a Barton differential pressure gage having a range of 0-100 inches of water.

The system pressure is maintained by the vapor pressure in an insulated pressure vessel heated by chromalox electric heaters.

EXPERIMENTAL TECHNIQUES

Determination of Temperatures at Liquid-Wall Interface. Because of mechanical problems it was impractical to measure the tube inner wall temperature directly. Instead, this temperature was calculated from measurements of the outer wall temperature, the electric current, and the geometrical and physical properties of the nickel tube.

The tube outer wall temperature was measured at seven points above the tube as shown in fig. 3 from twelve chromel-constantan thermocouples electrically insulated from the tube wall by a small sheet of 0.0015 in. thick mica. Around the tube was a copper shield electrically heated in three sections, each controlled by a variac. The space between the tube and the shield was filled with Kaolin wool insulation.

The shield temperature was adjusted to the same temperature as the test section thermocouple. Under such conditions the reading of the outer wall thermocouple can be considered to be the temperature of the tube outer wall.

In the surface boiling region the tube wall temperatures are fairly uniform; hence a uniform setting of shield temperatures for any one operating condition resulted in accurately determined wall temperatures. In the non-boiling region, the test section had an axial temperature gradient requiring adjustments of the three variacs to cause the shield to follow closely the tube temperatures.

A mock-up of the test section assembly (fig. 2) was tested with condensing steam in the test section to determine the effect of shield temperature variation on tube thermocouple reading. It was found that when the difference between steam temperature and shield temperature was 10°F, the difference between steam temperature and tube thermocouple temperature was between 1/2 and 1°F as recorded by the various thermocouples along the length. These differences varied approximately linearly with each other.

The inner wall temperature was calculated from a Taylor Series solution of the temperature distribution for heat conduction in an electrically heated tube with an adiabatic outer wall. This equation which is similar to that proposed by Kreith and Summerfield (1) is:

$$t_o - t_w = \frac{m}{k_o \rho_o}\left\{\overline{\Delta x}^2 + \frac{\overline{\Delta x}^3}{r_o} + \overline{\Delta x}^4\left[\frac{m}{6}\frac{(3\alpha + 4\alpha\beta t_o + \beta)}{(1+\beta t_o)(1+\alpha t_o)} + \frac{1}{4r_o^2} + \cdots \right.\right\} \quad (1)$$

where:
$$m \equiv \frac{3.412\, I^2 \rho_m^2}{2\pi^2 (r_o^2 - r_i^2)^2}$$

For accuracy within 0.5% the third term may be neglected, the working equation then becoming:

$$t_o - t_w = \frac{m}{k_o \rho_o}\left\{\overline{\Delta x}^2 + \frac{\overline{\Delta x}^3}{r_o} + \cdots\right\} \quad (1a)$$

This relation includes allowance for variation of electrical resistivity and thermal conductivity with temperature and for electrical resistivity with radius.

<u>Measurement of Heat-Flux Density</u>. The power dissipated in any portion of the test section is dependent upon the resistance, which, being a function of temperature, varies from point to point along the tube. The heat flux density then varies along the test section length and must be calculated to obtain accurate results. For a small element of length dx,

$$\frac{q}{A} = \frac{3.412\, I^2 \rho_m\, dx}{\pi D_i\, dx\, \pi (r_o^2 - r_i^2)} = 1.148 \times 10^6\, I^2 \rho_m \quad (2)$$

for the tube of 0.1805 in. I.D. and 0.2101 in. O.D.

The electric current was determined from the measured voltage drop across a 0.00001667 ohm G. E. manganin shunt calibrated by the National Bureau of Standards. The shunt was in series with the test section and its voltage drop was measured by a Rubicon potentiometer.

The voltage drop across the test section was measured by a potentiometer and a voltage divider network as illustrated in fig. 4. The resistors were General Radio Company resistors calibrated at the M.I.T. Electrical Instruments Laboratory. The potential taps were made of nickel held in place by stainless steel spring clips. The voltage drop across the test section is then

$$E_{ts} = E_1 \frac{R_1 + R_2 + R_3}{R_1} \tag{3}$$

Test Water Bulk Temperature. The method of determining the fluid temperature at any station along the tube consisted of integrating q/A from the inlet to the station in question and calculating the fluid temperature rise from the inlet. Neglecting axial heat flow and neglecting the effect of vapor bubbles on the effective specific heat of the water, an energy balance results in

$$\int_{\tau_{in}}^{\tau_n} d\tau = \frac{\pi D_i}{c_p w} \int_0^n \left(\frac{q}{A}\right) dx \tag{4}$$

For pusposes of graphical integration, a plot as shown in fig. 5 was made. In general it was sufficiently accurate to make the actual calculation by a stepwise integration between any two stations n and (n-1) in the form

$$\tau_n - \tau_{(n-1)} = \frac{\pi D_i}{w c_p} X_{n-(n-1)} (q/A)_{n-(n-1)} \tag{5}$$

Data from this apparatus affords several checks on itself. The average (q/A) calculated from the power measurement should be equal to the average (q/A) as calculated from equation (2). Also the sum of the water temperature rises between stations should equal $\tau_{out} - \tau_{in}$.

Flow Measurement. The pressure drop across the orifice was measured with Barton Differential Pressure Gages with 0-100" H_2O scale. Its accuracy calibrated at atmospheric pressure against a water column was within 1% of full scale reading. The orifice coefficient calibrated by direct weighing at eight Reynolds numbers for pressure drop readings from 10 to 90" H_2O had a root-mean-square deviation of 0.5% for the high flow range orifice and 0.9% for the low range orifice. The accuracy of the flow measurement should be within 1 per cent.

Test-Section Pressure Drop Measurement. Pressure drop across the test section is measured by means of a Barton Differential Pressure Gage, 0-300 inches of water, connected at the pressure taps as shown in Fig. 2. The pressure drop, Δp_i, across the heated section was determined from corrected gage reading by subtracting the pressure drops in the unheated sections at either end of the tube as determined from isothermal friction factors. The temperature of the water in the vertical test section is considerably higher than the temperature of the ambient water in the gage lead-in tubing, necessitating a correction factor to determine the actual pressure drop due to friction and momentum change. The equation relating these pressure drop values is as follows:

$$\Delta p_{f,m} = \Delta p_i + L_p(\gamma_0 - \bar{\gamma}) \qquad (6)$$

Because of the addition of heat to the fluid its density changed in passing through the test section. This resulting momentum change must be subtracted from $\Delta p_{f,m}$ to obtain the pressure drop associated with friction alone. Then

$$\Delta p_f = \Delta p_{f,m} - \frac{G^2}{g_0}\left(\frac{1}{\rho_2} - \frac{1}{\rho_1}\right) \qquad (7)$$

A friction factor based on the friction pressure drop may be defined by the equation

$$\Delta p_f = 4 f_f \frac{G^2}{2 g_0 D_i} \int_0^L \frac{dx}{\rho} \qquad (8)$$

and when based on the pressure drop including both frictional and momentum effects

$$\Delta p_{f,m} = 4 f_{f,m} \frac{G^2}{2 g_0 D_i} \int_0^L \frac{dx}{\rho} \qquad (9)$$

In each case the actual variation of density along the tube length was used in evaluating the integral.

Accuracy of Results. The tube thickness varied ± 0.0003 in. Equation (2) with the value of m introduced shows the first and major term of the series to be approximately inversely proportional to the square of the tube diameter. For the high heat flux tests the value of $T_o - T_w$ was about 60°F; then the maximum error of T_w attributable to tube thickness variation was 0.4°F and decreases as the heat flux is lowered.

The thermal conductivity data was obtained from the International Nickel Company and the electrical resistivity was determined experimentally to an estimated accuracy of ± 0.5%.

It is expected that the inner-wall temperature has been determined within a ± 3 degree F error.

ION EXCHANGER

During early test runs black iron oxide was found to be depositing in the test section causing as much as a 50°F increase in tube wall temperature in two hours of operation at a fixed set of conditions. The source of iron ions was probably the Hayward-Tyler pump which, contrary to expectations, had a considerable amount of ordinary iron in contact with the test water. It was suggested that the deposit was formed because of the electrical potential gradient along the test water in the tube and the ions (hence electrical conductivity) of the test water. A mono-bed ion exchanger consisting of Rohn and Haas Resin MB-1 "Amberlite" in a stainless steel jacket equipped with suitable filters was added to the circuit as shown in figure 1. It is not as yet known whether this ion-exchanger actually removed the objectionalbe ions or simply acted as a high grade filter, but subsequent to its installation all difficulty with deposition of scale on the heat transfer surface ceased.

EXPERIMENTAL PROCEDURE

The system was filled with freshly distilled water (0.70 ppm as NaCl and approximately 15 ml air/l) by means of an aspirator located at the top of the Hayward-Tyler pump. As soon as it was certain that the upper thrust bearing on the Hayward-Tyler pump was immersed in water, the pump was started and water was circulated through the test loop. Degassing was accomplished by circulating the test circuit water through the heated pressure vessel vented to the atmosphere for a period of 1/2 to 3/4 of an hour. This period was found to be of sufficient length to reduce the oxygen content to approximately 1.5 ml air/l, as determined by the Winkler Technique. Subsequent to degassing, the system was sealed by closing the degassing vent valve and test water was circulated through the test section at high velocity. The bulk temperature of the water was increased by applying power to the test section and the system pressure was increased to the desired level by heating the water in the closed pressure vessel. The system pressure could be controlled to ± 2 psi by the chromalox strip heaters regulated by a variac. The inlet bulk temperature was controlled and maintained at the desired level by regulating the flow of silicone fluid through the intermediate heat exchanger. Cooling water flow through the ion-exchanger heat exchanger and the city water heat exchanger was fixed at its maximum rate at the beginning of the run and not thereafter adjusted. The water at the discharge of the ion-exchanger was consistently at approximately 0.1 ppm NaCl.

EXPERIMENTAL RESULTS

Heat Transfer in Forced Convection Without Surface Boiling.

Local values of the heat transfer coefficient at stations 2 through 6 (Fig. 3) were evaluated by assuming a linear variation of fluid temperature with distance along the tube. The tube wall temperature varied along the tube in the non-boiling runs; so q/A was not uniform because the wall electrical resistivity varies with temperature. Nevertheless the assumption of linear fluid temperature resulted in at most a 3% error in the resulting local heat transfer coefficient for runs involving high rates of heat transfer at lower velocities.

The results of these runs are shown in Table I and figure 6. The local value of j is shown plotted against the local N_{Ref}. It is noted that there exists a separate curve for the points along the tube for each run and the points near the end of the tube are correlated by the equation

$$\frac{h}{c_p G}\left(\frac{c_p \mu_f}{k}\right)^{2/3} = 0.019\left(\frac{G D_i}{\mu_f}\right)^{-0.2} \tag{10}$$

which is below the Colburn correlation line by about 17%. The values of the heat transfer coefficient at the points toward the inlet end of the tube are higher than the correlation line which is drawn for the points near the outlet end of the tube. This is to be expected because of the build up of the thermal boundary layer. The tube has an L/d of 52. For most cases an L/d of approximately 50 is found to be necessary to form a fully developed thermal boundary layer; hence, the trend of the data seems to be reasonable.

There is, of course, the possibility that a film of contamination on the heat transfer surface would result in too high a temperature difference and thus reduce the j value. However, this effect is discounted as being negligible since it would have to account for an interface temperature error of from 20°F to 40°F to bring the correlation in line with the Colburn correlation. Doubtless the film exists since examination of used tubes showed a slight discoloring of the heat transfer surface. It was extremely thin, however, reflecting incident light as blue suggesting its thickness as the order of the wave length of that color light. Also, inspection of Fig. 8 shows that if the true Δt is as much as 10°F below that reported then boiling would occur at temperatures less than saturation, which is improbable.

Energy balances comparing enthalpy change of liquid with the electrical energy were all within ± 2 %, most of them being within ± 0.5%. Isothermal runs with the liquid temperatures above 400°F showed the inlet and outlet liquid thermocouple to agree within ± 1°F of the tube wall temperatures.

The values of the fluid properties were obtained from data taken from Wellman (8).

Heat Transfer in Forced Convection with Surface Boiling

Again local values of q/A as a function of temperature difference are studied. In these boiling runs the tube temperature, and hence q/A, is very nearly uniform along the tube. The temperature of the fluid is assumed to vary linearly with distance along the tube. This assumption is not strictly valid for conditions of high heat flux or heat transfer to a liquid with low subcooling where the percentage of volume occupied by vapor becomes significant. Since the effect of these vapor bubbles on bulk temperature changes could not be determined from the measurements taken it was assumed the fluid behaved as a liquid and as a check on the assumption the longitudinal variation in bulk enthalpy and thus bulk temperature was determined by a numerical integration of q/A with length. The results agreed within 2°F of the assumed linear variation.

Figure 7 illustrates the type of information obtained from a set of runs. Five data points are obtained for a run, each at nearly the same q/A value but a different value of liquid subcooling. Similar curves for other conditions are shown in figures 13 through 17 from the data in Tables I and II.

The curves of figure 7 for various values of subcooling can be brought together to fall on a single line by plotting q/A vs. $(t_w - t_{sat.})$, the wall superheat, as shown in figure 8. Here data in the region of surface boiling (Table II) are plotted for various values of fluid velocities and pressures. The points plotted here are the average values of the five points along the tube for each run. The value of q/A along the tube did not vary significantly but the value of $(t_w - t_{sat})$ varied within ± 2°F from the mean value plotted. It is observed that at these high pressures the amount of wall superheat is very small, generally less than 10°F at 2000 psia and less than 15°F at 1500 psia. At lower values of pressure near atmospheric Kreith and Summerfield (1) found values of wall superheat to be around 60°F. Errors in the smaller values of wall superheat are magnified on the log-log type of plot in figure 8. The uncertainties of ± 2 or 3°F in wall temperature values have greater emphasis here. These discrepancies when referred to the value of $(t_w - t_b)$ are very small, however.

The general trend of the curves of figure 8 shows the same effect reported by previous investigators (1), (2), (3), and (4) in the lower pressure range, e.g., at the higher heat transfer rates the effect of fluid velocity decreases and the agitation of the fluid by the bubbles governs the rate of heat transfer and at the higher pressures less wall superheat exists at a given rate of heat transfer.

Pressure Drop in Forced Convection Without Surface Boiling

Local values of pressure drop could not be obtained because such measurements would interfere with the heat transfer measurements; hence, overall values of pressure drop were obtained and are tabulated in Table III, and friction factors are shown in figure 9 as a function of bulk Reynolds number at the arithmetic mean value of inlet and outlet fluid temperatures. The f_f and $f_{f,m}$ values are shown compared with the isothermal values found in figure 51 of McAdams (5).

In figure 10 the ratio of isothermal friction factor to the friction factor with heat transfer is plotted as a function of (μ_b/μ_w) at the arithmetic mean value of inlet and outlet fluid temperatures. The ratio involving $f_{f,m}$ is seen to correlate with the generally accepted line having a slope of 0.14, but the ratio involving f_f is correlated with a line having a slope of 0.60 for these data.

Pressure Drop in Forced Convection With Surface Boiling

Data of Table IV is plotted in figures 11 and 12 and show the effect of heat flux on the pressure drop quantities for friction alone and for friction plus momentum change. When surface boiling begins the pressure drop begins to rise slightly as q/A is increased. A velocity effect and an effect of liquid subcooling or absolute pressure is observed. It appears that the effect of liquid subcooling is more pronounced than the effect of absolute pressure.

Since five local values of heat transfer coefficients were obtained for each value of overall pressure drop there is much less pressure drop data available. Generally one particular range of liquid subcooling values was associated with particular values of absolute pressure and velocity. At 2000 psia and 20 ft/sec most of the data were taken with a mean subcooling of around 160°F; however, two runs were made at a liquid subcooling of around 237°F. The curves drawn through points indicate that the effect on pressure drop of liquid subcooling is probably more important than the effect of absolute pressure in ranges of these tests. More test data is needed to explore more fully this effect.

Summary of Results

1. For fully developed flow the non-boiling heat transfer data at 1500 psia and 2000 psia is correlated by the equation

$$\frac{h}{c_p G}\left(\frac{c_p \mu_f}{k}\right)^{2/3} = 0.019\left(\frac{G D_i}{\mu_f}\right)^{-0.2}$$

2. With surface boiling the heat transfer data plotted against $(t_w - t_{sat})$, wall superheat, shows a principal effect due to absolute pressure and a secondary effect due to fluid velocity. At high q/A values the wall superheat becomes nearly independent of fluid velocity and decreases as pressure increases.

3. For non-boiling heat transfer the friction factors may be correlated by

$$\frac{f_{(isothermal)}}{f_{f,m}} = \left(\frac{\mu_b}{\mu_w}\right)^{0.14}$$

$$\frac{f_{(isothermal)}}{f_f} = \left(\frac{\mu_b}{\mu_w}\right)^{0.60}$$

4. With surface boiling the pressure drop increases with increasing heat flux and decreasing subcooling and decreasing pressure.

Acknowledgements

The work reported here was sponsored by the Office of Naval Research, Contract N5-ori-07827, NR-035-267. The authors gratefully acknowledge this aid and also the help of the following persons. The many problems associated with the design of the high pressure apparatus were for the most part solved by Mr. Milton W. Raymond, project design engineer, who also originally conceived and successfully built the ion-exchanger with very little design data. The maintenance and operation of the equipment and the gathering of the test data was accomplished by Messrs. William W. Barton, Edward H. Somma, Paul V. Osborn, Francis J. Zimmerman and Frank Mullin, graduate students in the Department of Mechanical Engineering, Massachusetts Institute of Technology.

Bibliography

1. Kreith, F. and Summerfield, M., "Heat Transfer to Water at High Flux Densities With and Without Surface Boiling," A.S.M.E. Trans., Vol. 71, No. 7, p. 805, Oct., 1949.

2. Kreith, F. and Summerfield, M., "Pressure Drop and Convective Heat Transfer with Surface Boiling at High Heat Flux; Data for Aniline and n-Butyl Alcohol," A.S.M.E. Trans., Vol. 72, No. 6, p. 869, Aug., 1950.

3. Knowles, J. W., "Heat Transfer With Surface Boiling," Canadian Journal of Research, 26A, 268-278, 1948.

4. McAdams, W. H., Kennel, W. E., Minden, C. S., Rudolf, C., Picornell, P. M., Dew, J. E., "Heat Transfer at High Rates to Water With Surface Boiling," Ind. and Eng. Chem., Vol. 41, p. 1945, Sept., 1949.

5. McAdams, W. H., Heat Transmission, McGraw-Hill, 1942.

6. Rohsenow, W. M., Somma, E. H., Osborn, P. V., "Construction and Operation of Apparatus for Study of Heat Transfer with Surface Boiling," Tech. Report No. 2, D.I.C. Project No. 6627, Mass. Inst. of Tech., July, 1950.

7. Clark, J. A. and Rohsenow, W. M., "Statement of Progress for Period 23 July 1950 to 1 September 1950," D.I.C. Project No. 6627, Mass. Inst. of Tech.

8. Wellman, E. J., "A Survey of the Thermodynamic and Physical Properties of Water," M. S. Thesis, Purdue University, 1950.

9. Rohsenow, W. M., and Clark, J. A., "Heat Transfer and Pressure Drop Data for High Heat Flux Densities to Water at High Subcritical Pressures," Heat Transfer and Fluid Mechanics Institute, Stanford, California, June, 1951.

10. Buchberg, H., Romie, F., "Heat Transfer, Pressure Drop, and Burnout Studies With and Without Surface Boiling For De-Aerated and Gassed Water at Elevated Pressures in a Forced Flow System," Heat Transfer and Fluid Mechanics Institute, Stanford, California, June, 1951.

Nomenclature

A	Heat transfer area, sq feet
c_p	Specific heat, Btu/lb °F
D_i	Inner diameter of test section, feet
E	Test section voltage, volts
G	Mass velocity, lb/hr ft^2
h	Surface coefficient of heat transfer, Btu/hr ft^2°F
I	Test section current, amperes
k	Thermal conductivity of fluid, Btu/hr ft °F
k_o	Thermal conductivity of tube wall at t_o, Btu/hr ft °F
L_p	Test section heated length, ft
$N_{Re,f}$	$= \frac{D_i G}{\mu_f}$
P	Pressure, psia
ΔP_i	Pressure drop reading across test section, in. H_2O
$\Delta P_{f,m}$	Pressure drop due to friction and momentum change, in. H_2O
ΔP_f	Pressure drop due to friction alone
q/A	Heat flux density, Btu/hr ft^2
$(q/A)_{n-(n-1)}$	$= \frac{1}{2}\left[(q/A)_n + (q/A)_{(n-1)}\right]$
f_f	Defined by eq. (8)
$f_{f,m}$	Defined by eq. (9)
j	$= \frac{h}{c_p G}\left(\frac{c_p \mu_f}{k}\right)^{2/3}$
r_o	Outer radius of test section, feet
r_i	Inner radius of test section, feet
R	Resistance, ohms
τ_b	Test water bulk temperature, °F
τ_{in}	Test water inlet bulk temperature, °F
τ_{out}	Test water outlet bulk temperature, °F
t_o	Test section outer wall temperature, °F

t_w	Test section inner wall temperature, °F
t_{sat}	Saturation temperature, °F
T_x	Wall temperature minus saturation temperature, $t_w - t_{sat}$, °F
V	Flow velocity, feet/sec
w	Flow rate, lb/hr
Δx	$= (r_o - r_i)$
x	Distance between thermocouple stations, 1.4 inches
β	Temperature coefficient of electrical resistivity, $°F^{-1}$
α	Temperature coefficient of thermal conductivity, $°F^{-1}$
$\bar{\gamma}$	Mean density of fluid in test section, lb_f/cu ft
γ_o	Density of liquid in lead lines to pressure gage, lb_f/cu ft
ρ_o	Electrical resistivity at t_o, ohm feet
ρ_m	Electrical resistivity at temperature $t_m = \frac{1}{\Delta x}\int_{r_i}^{r_o}(t - t_w)\,dr$
ρ	Mass density of fluid at fluid temperature, lb_m/cu ft
μ_f	Viscosity at film temperature, $\frac{\tau_b + t_w}{2}$, lb/hr ft

Figure Captions

1. Layout of Test Apparatus
2. Test Section Assembly
3. Location of Thermocouples and Potential Taps
4. Test Section Voltage Measurement
5. Heat Flux Density and Bulk Temperature Along the Tube, Non-Boiling Run
6. j-Factor vs. Reynolds Number for Forced Convection Without Surface Boiling
7. Heat Flux vs. Temperature Difference for Forced Convection with Surface Boiling of Water at 2000 psia and 20 ft/sec Inlet Velocity
8. Heat Flux vs. Wall Superheat for Forced Convection with Surface Boiling
9. Friction Factor vs. Reynolds Number for Forced Convection without Surface Boiling
10. Correction Factor for Friction Factor with Heat Transfer Without Surface Boiling
11. Effect of Heat Flux on $\Delta P_{f,m}$
12. Effect of Heat Flux on ΔP_f
13. Heat Flux vs. Temperature Difference for Forced Convection with Surface Boiling of Water at 2000 psia and 30 ft/sec Inlet Velocity
14. Heat Flux vs. Temperature Difference for Forced Convection with Surface Boiling of Water at 2000 psia and 10 ft/sec Inlet Velocity
15. Heat Flux vs. Temperature Difference for Forced Convection with Surface Boiling of Water at 1500 psia and 30 ft/sec inlet Velocity
16. Heat Flux vs. Temperature Difference for Forced Convection with Surface Boiling of Water at 1500 psia and 20 ft/sec Inlet Velocity
17. Heat Flux vs. Temperature Difference for Forced Convection with Surface Boiling of Water at 1500 psia and 10 ft/sec Inlet Velocity

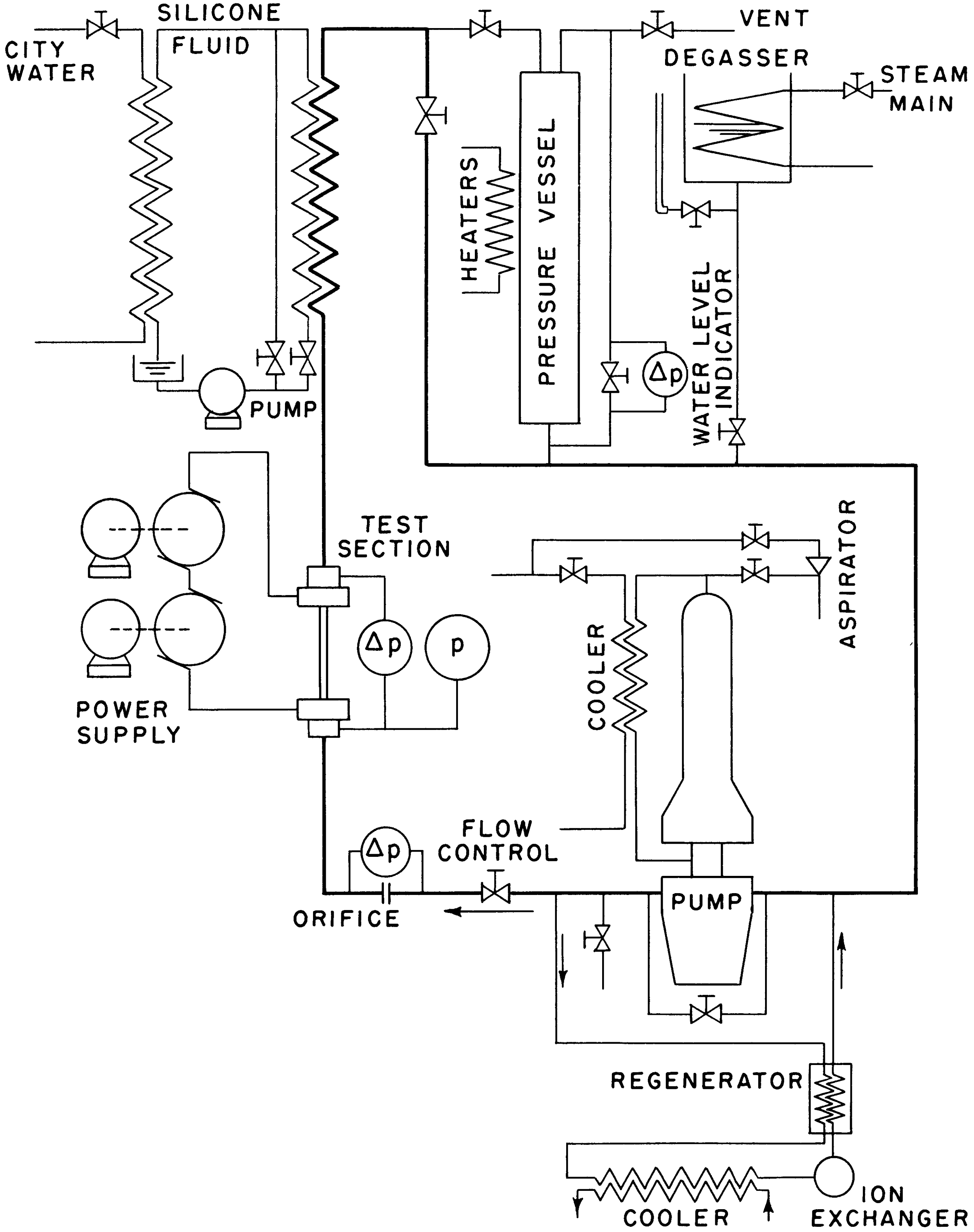

LAYOUT OF TEST APPARATUS

FIGURE I

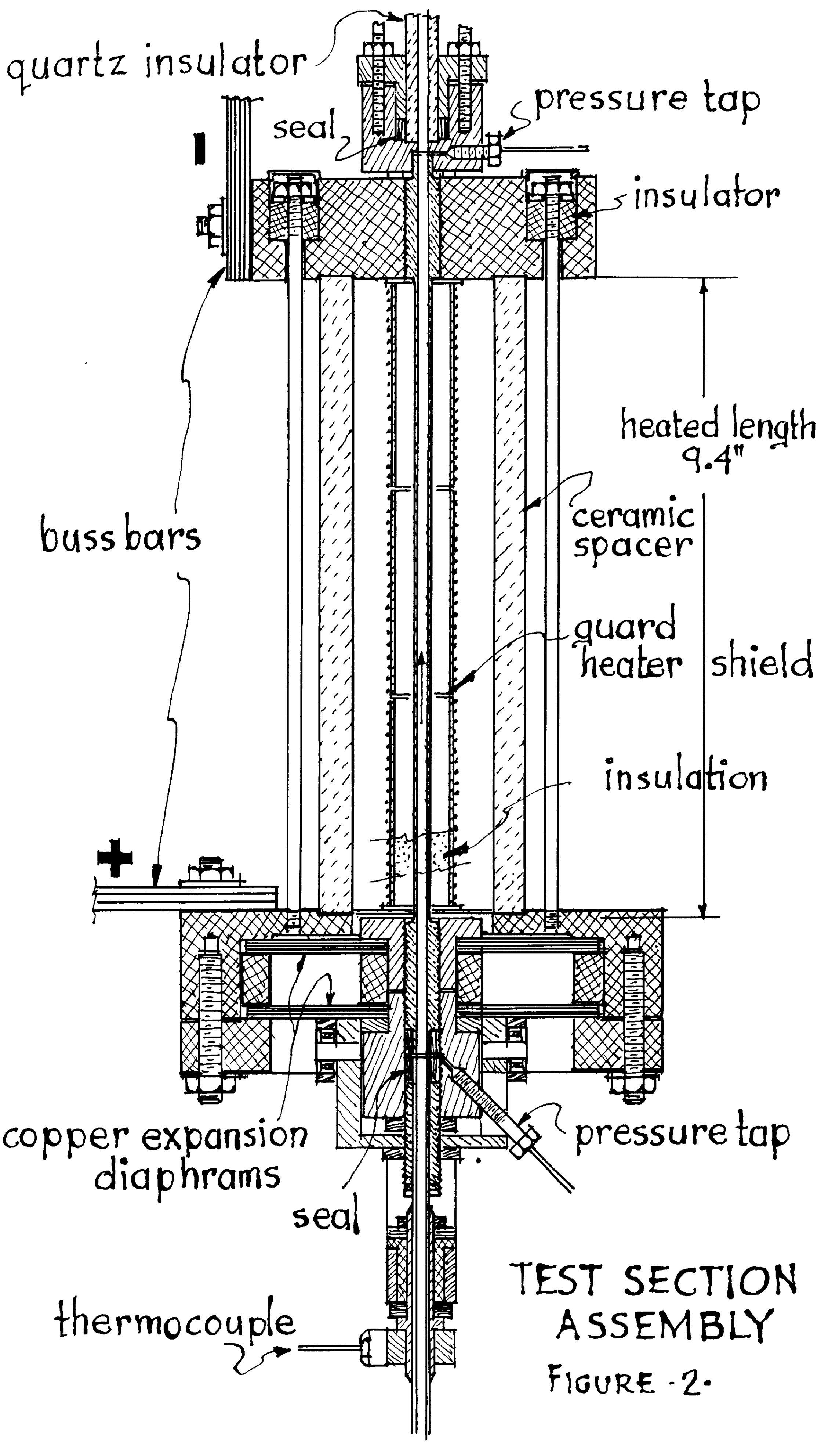

TEST SECTION
ASSEMBLY

FIGURE -2-

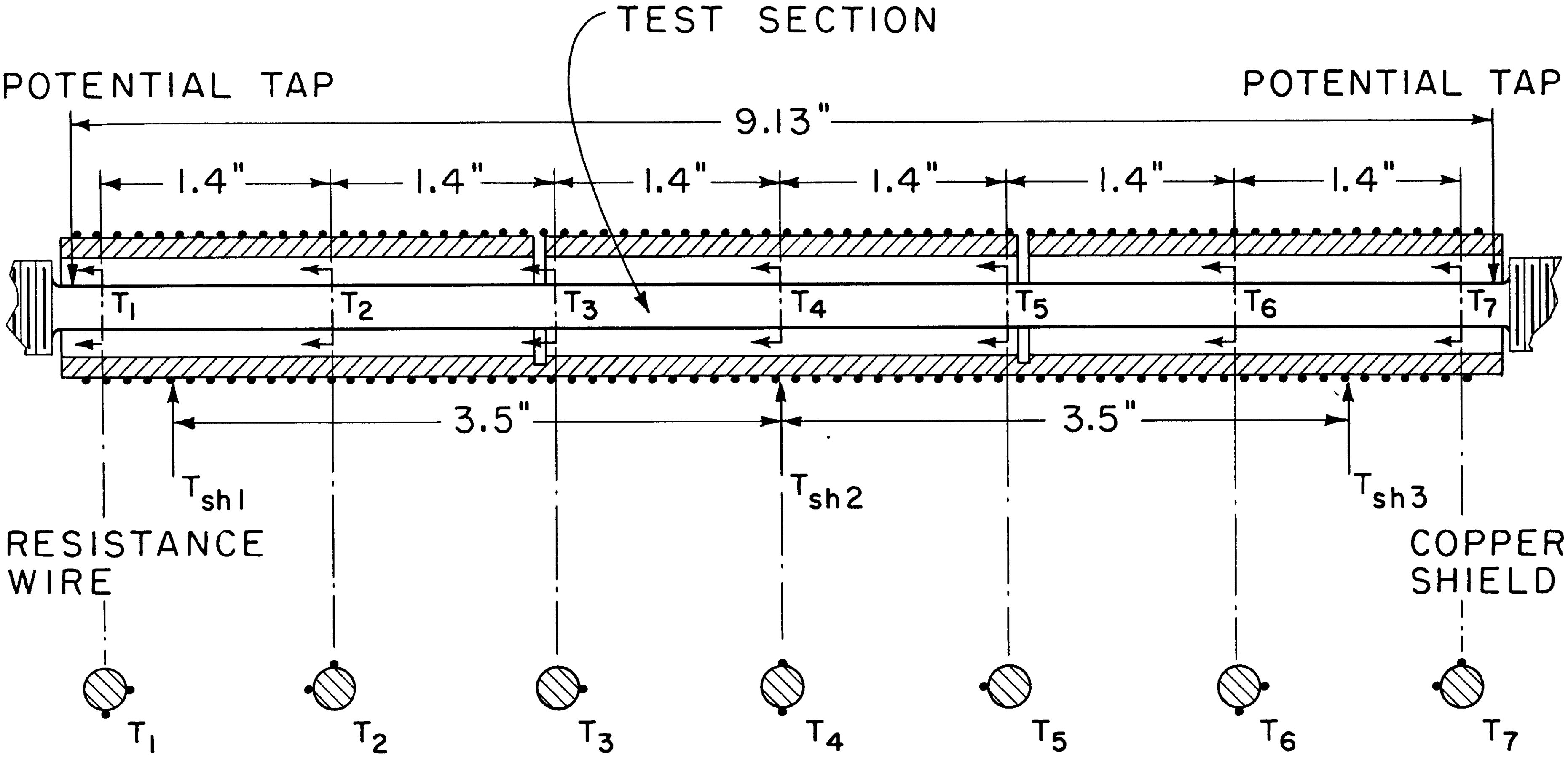

LOCATION OF THERMOCOUPLES AND POTENTIAL TAPS

FIGURE 3

TEST SECTION VOLTAGE MEASUREMENT

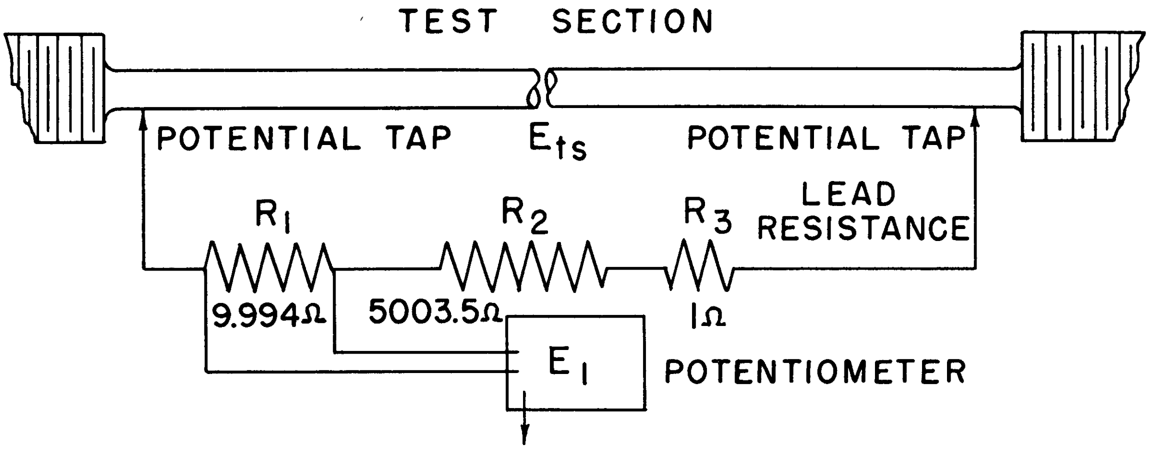

FIGURE 4

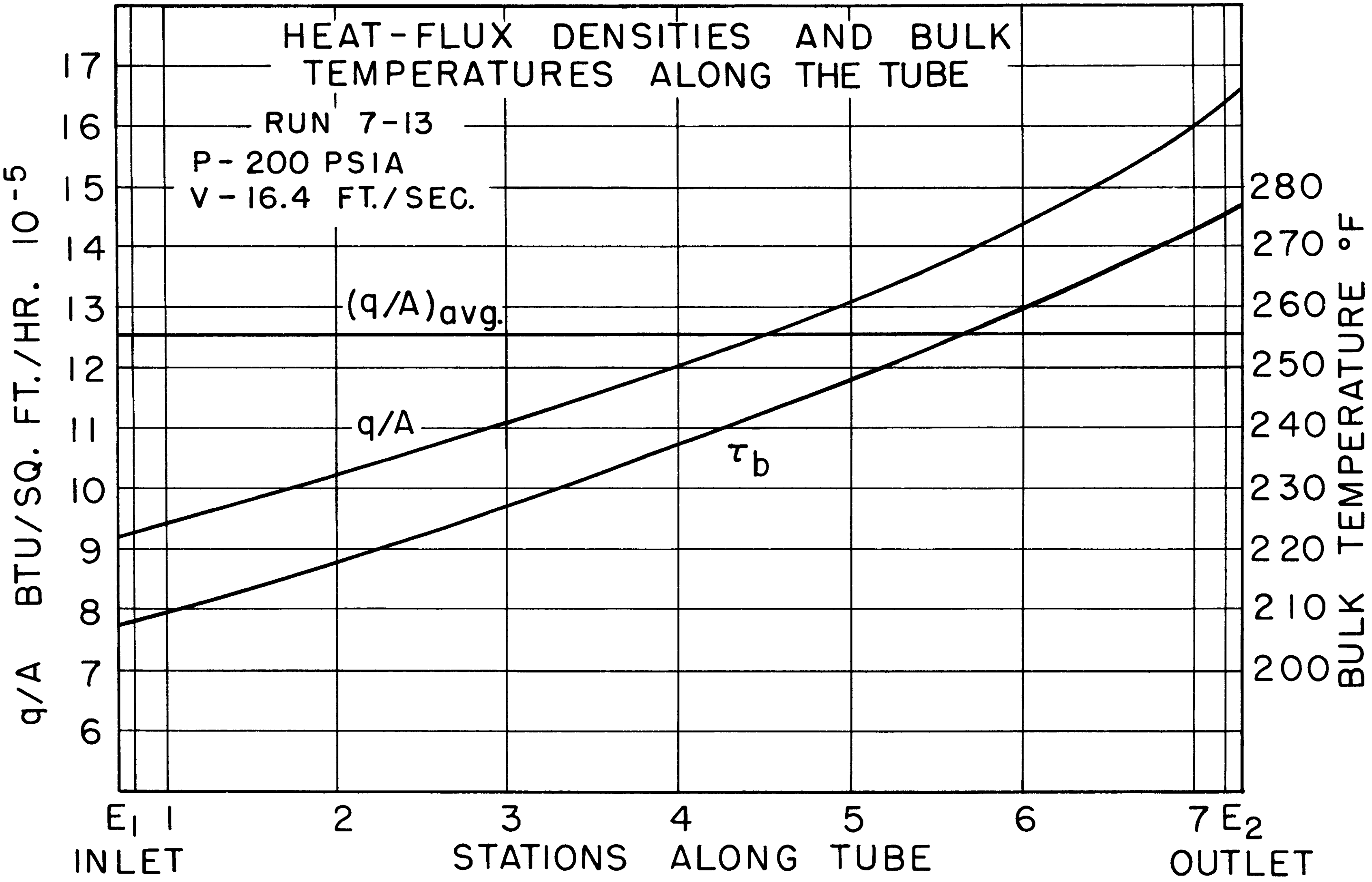
HEAT-FLUX DENSITIES AND BULK TEMPERATURES ALONG THE TUBE
RUN 7-13
P - 200 PSIA
V - 16.4 FT./SEC.
(q/A)avg.
q/A
τb
q/A BTU/SQ. FT./HR. 10-5
6
7
8
9
10
11
12
13
14
15
16
17
BULK TEMPERATURE °F
200
210
220
230
240
250
260
270
280
E1 1
2
3
4
5
6
7 E2
INLET
STATIONS ALONG TUBE
OUTLET

FIGURE 5

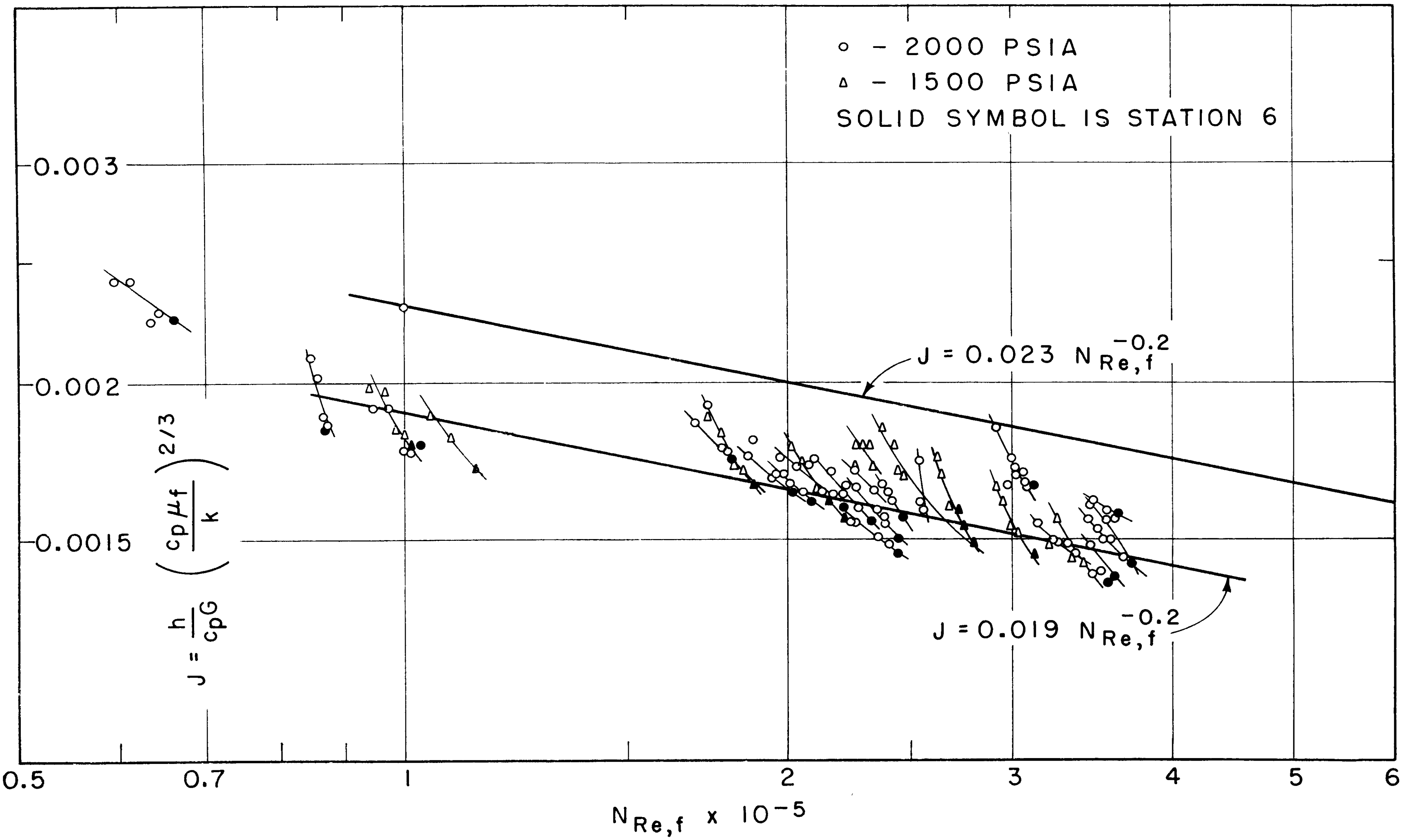
○ - 2000 PSIA
△ - 1500 PSIA
SOLID SYMBOL IS STATION 6
$J = 0.023\ N_{Re,f}^{-0.2}$
$J = 0.019\ N_{Re,f}^{-0.2}$
0.003
0.002
0.0015
$J = \frac{h}{c_pG}\left(\frac{c_p\mu_f}{k}\right)^{2/3}$
0.5
0.7
1
2
3
4
5
6
$N_{Re,f} \times 10^{-5}$

FIGURE 6

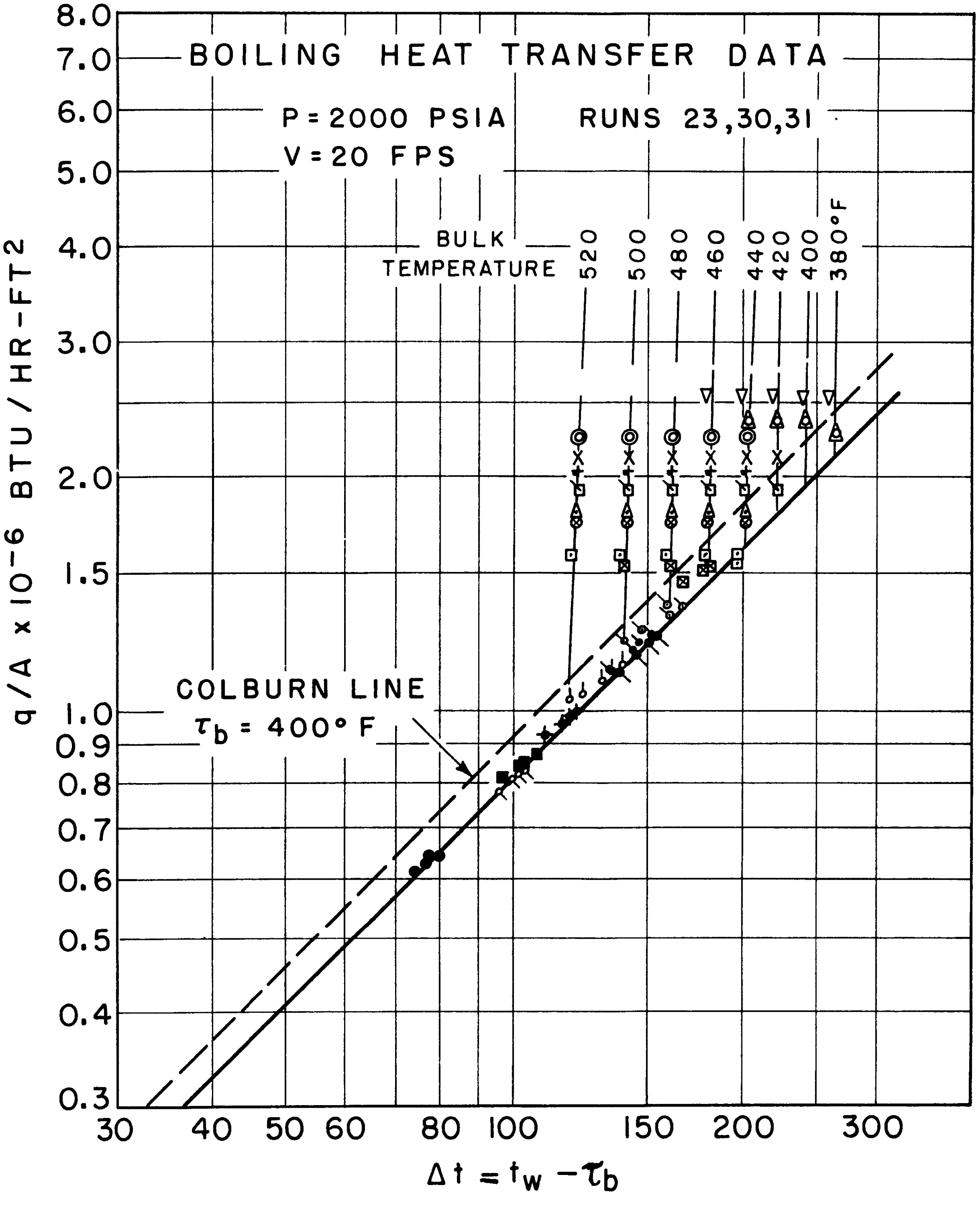
BOILING HEAT TRANSFER DATA
P = 2000 PSIA
V = 20 FPS
RUNS 23,30,31
BULK TEMPERATURE
520
500
480
460
440
420
400
380°F
COLBURN LINE
τ_b = 400° F
$q/A \times 10^{-6}$ BTU / HR-FT2
8.0
7.0
6.0
5.0
4.0
3.0
2.0
1.5
1.0
0.9
0.8
0.7
0.6
0.5
0.4
0.3
30
40
50
60
80
100
150
200
300
$\Delta t = t_w - \tau_b$

FIGURE 7

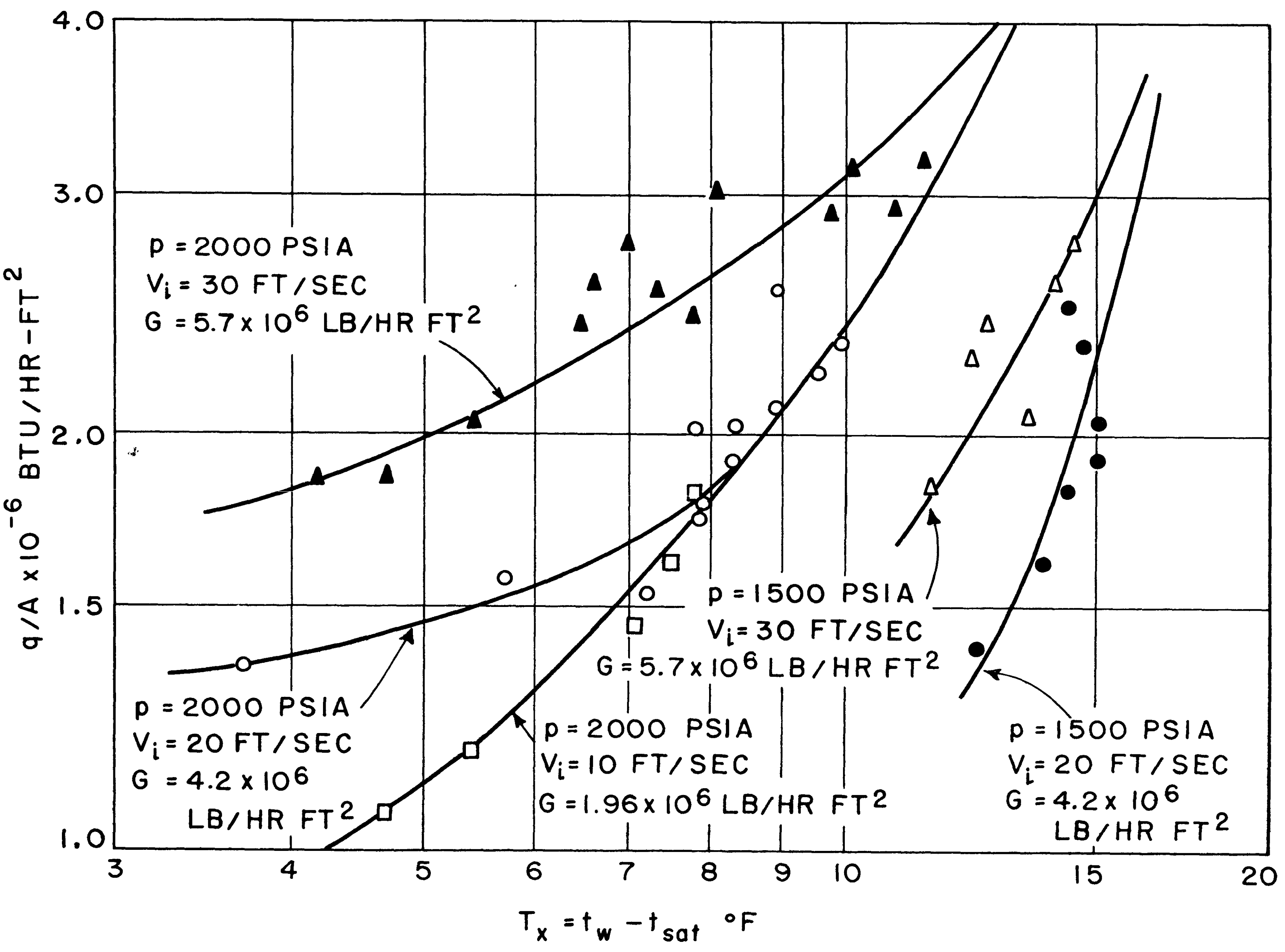
4.0
3.0
2.0
1.5
1.0
$q/A \times 10^{-6}$ BTU/HR-FT^2
3
4
5
6
7
8
9
10
15
20
$T_x = t_w - t_{sat}$ °F
p = 2000 PSIA
V_i = 30 FT/SEC
G = 5.7 x 10^6 LB/HR FT^2
p = 2000 PSIA
V_i = 20 FT/SEC
G = 4.2 x 10^6
LB/HR FT^2
p = 2000 PSIA
V_i = 10 FT/SEC
G = 1.96 x 10^6 LB/HR FT^2
p = 1500 PSIA
V_i = 30 FT/SEC
G = 5.7 x 10^6 LB/HR FT^2
p = 1500 PSIA
V_i = 20 FT/SEC
G = 4.2 x 10^6
LB/HR FT^2

FIGURE 8

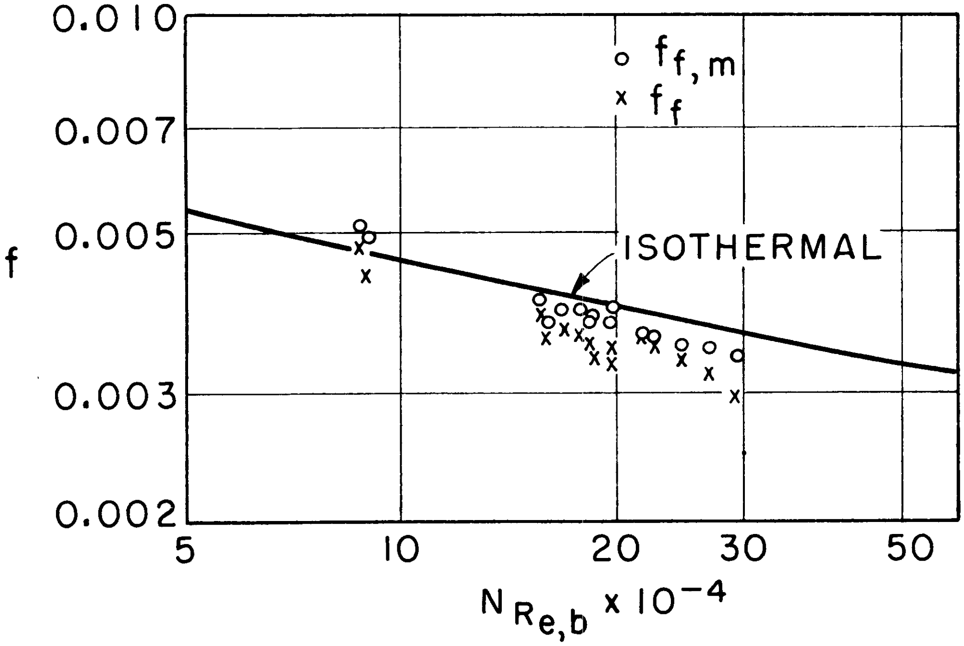

0.010
0.007
0.005
0.003
0.002
f
5
10
20
30
50
$N_{Re,b} \times 10^{-4}$
o $f_{f,m}$
x f_f
ISOTHERMAL

FIGURE 9

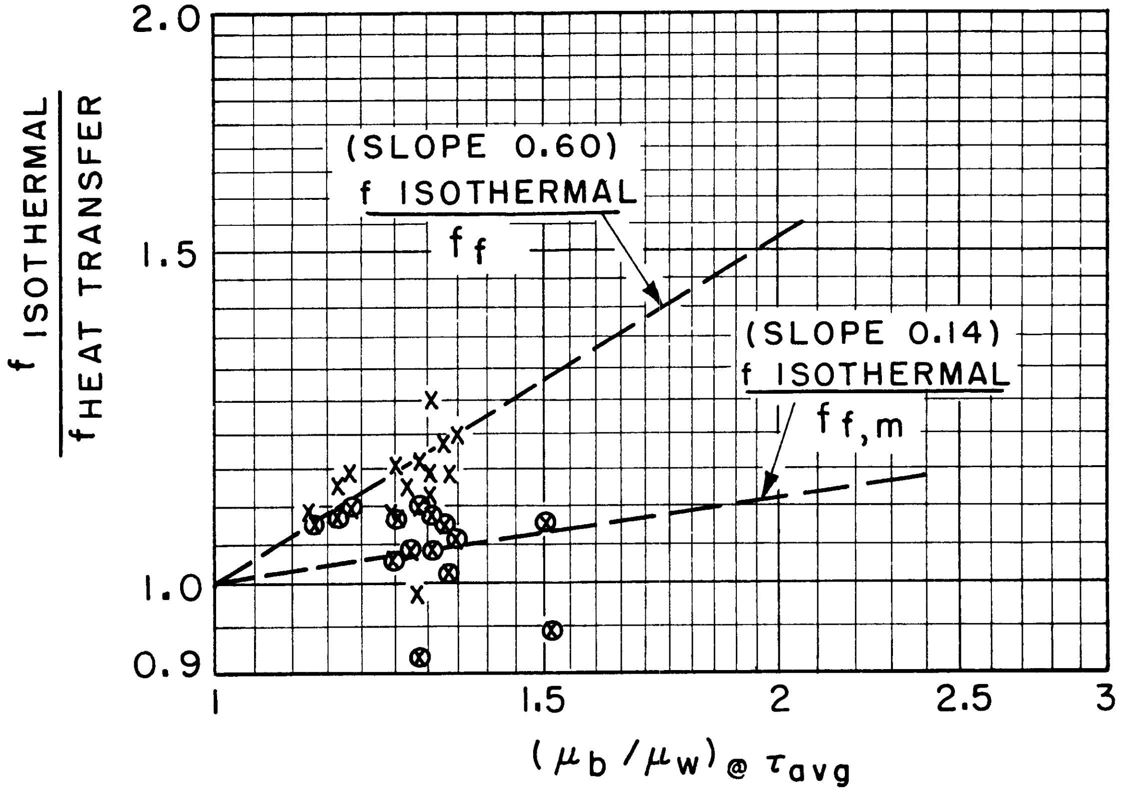
2.0
1.5
1.0
0.9
f ISOTHERMAL / f HEAT TRANSFER
(SLOPE 0.60)
f ISOTHERMAL / f f
(SLOPE 0.14)
f ISOTHERMAL / f f,m
1
1.5
2
2.5
3
$(\mu_b/\mu_w)_{@\,\tau_{avg}}$

FIGURE 10

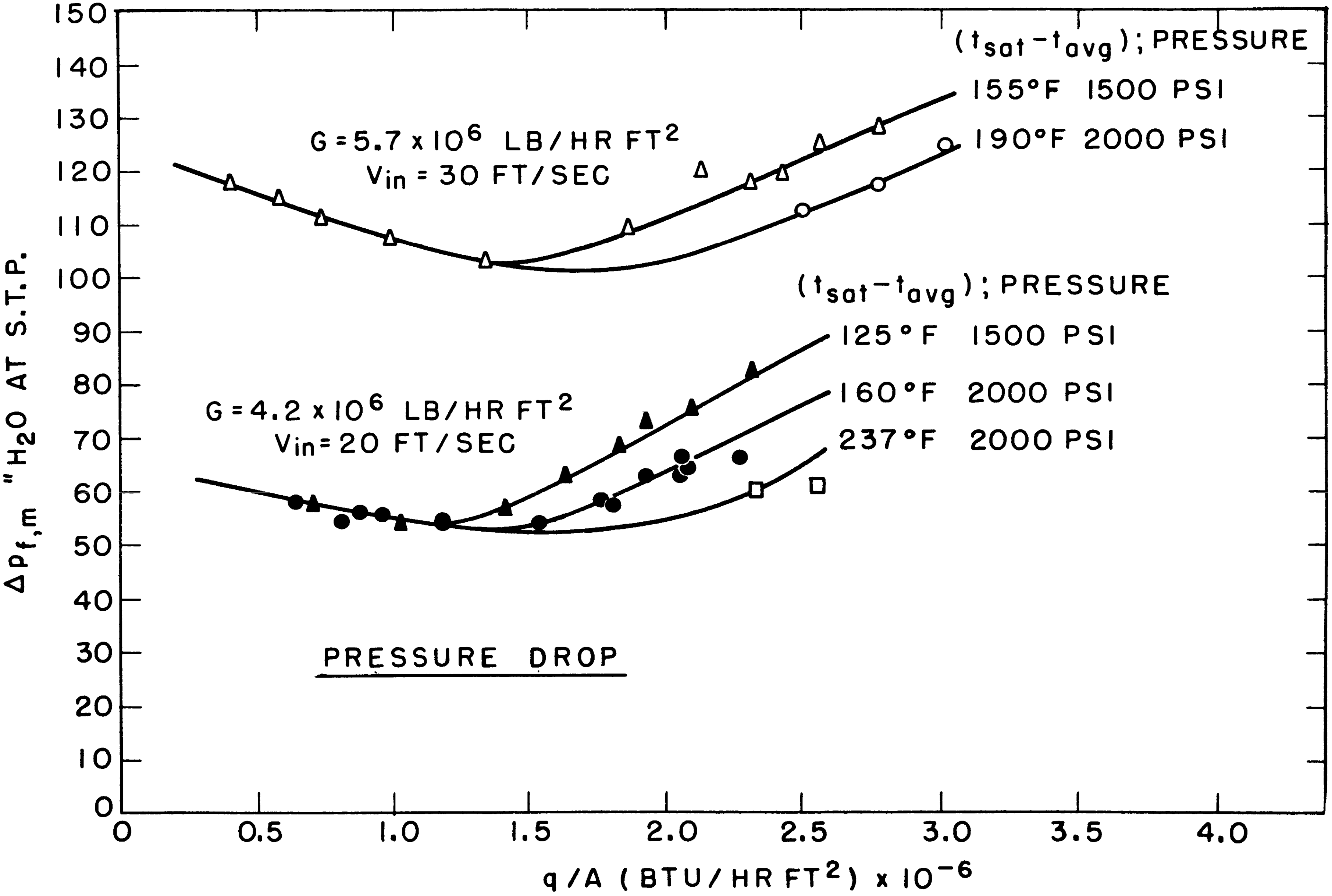

150
140
130
120
110
100
90
80
70
60
50
40
30
20
10
0
0
0.5
1.0
1.5
2.0
2.5
3.0
3.5
4.0
$\Delta P_{f,m}$ "H_2O AT S.T.P.
q/A (BTU/HR FT^2) x 10^{-6}
$G = 5.7 \times 10^6$ LB/HR FT^2
V_{in} = 30 FT/SEC
($t_{sat} - t_{avg}$); PRESSURE
155°F 1500 PSI
190°F 2000 PSI
$G = 4.2 \times 10^6$ LB/HR FT^2
V_{in} = 20 FT/SEC
($t_{sat} - t_{avg}$); PRESSURE
125°F 1500 PSI
160°F 2000 PSI
237°F 2000 PSI
PRESSURE DROP

FIGURE 11

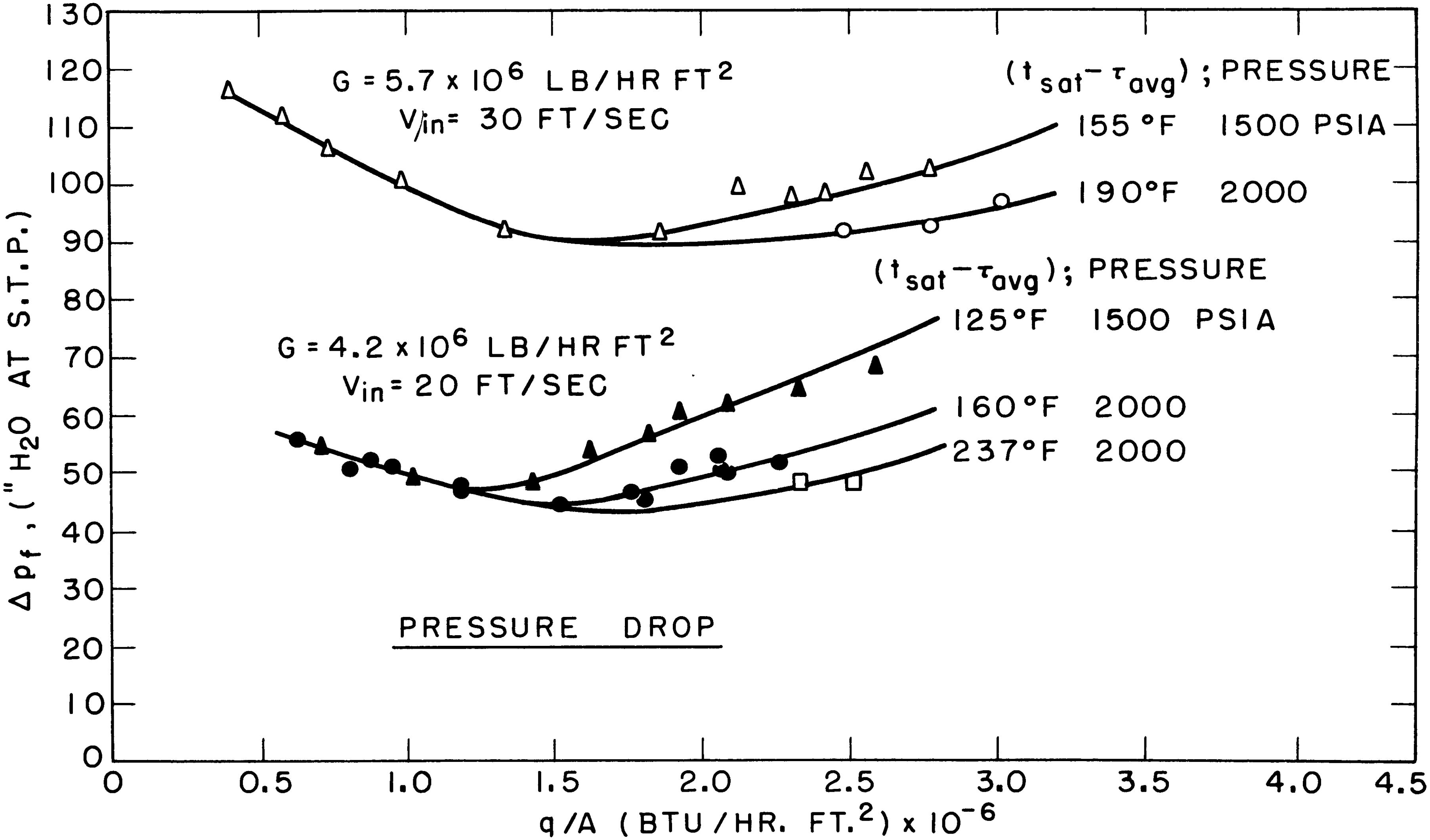

130
120
110
100
90
80
70
60
50
40
30
20
10
0
Δp_f, ("H_2O AT S.T.P.)
G = 5.7 x 10^6 LB/HR FT^2
V_{in} = 30 FT/SEC
($t_{sat} - \tau_{avg}$) ; PRESSURE
155 °F 1500 PSIA
190°F 2000
($t_{sat} - \tau_{avg}$); PRESSURE
125°F 1500 PSIA
G = 4.2 x 10^6 LB/HR FT^2
V_{in} = 20 FT/SEC
160°F 2000
237°F 2000
PRESSURE DROP
0
0.5
1.0
1.5
2.0
2.5
3.0
3.5
4.0
4.5
q/A (BTU/HR. FT.^{2}) x 10^{-6}

FIGURE 12

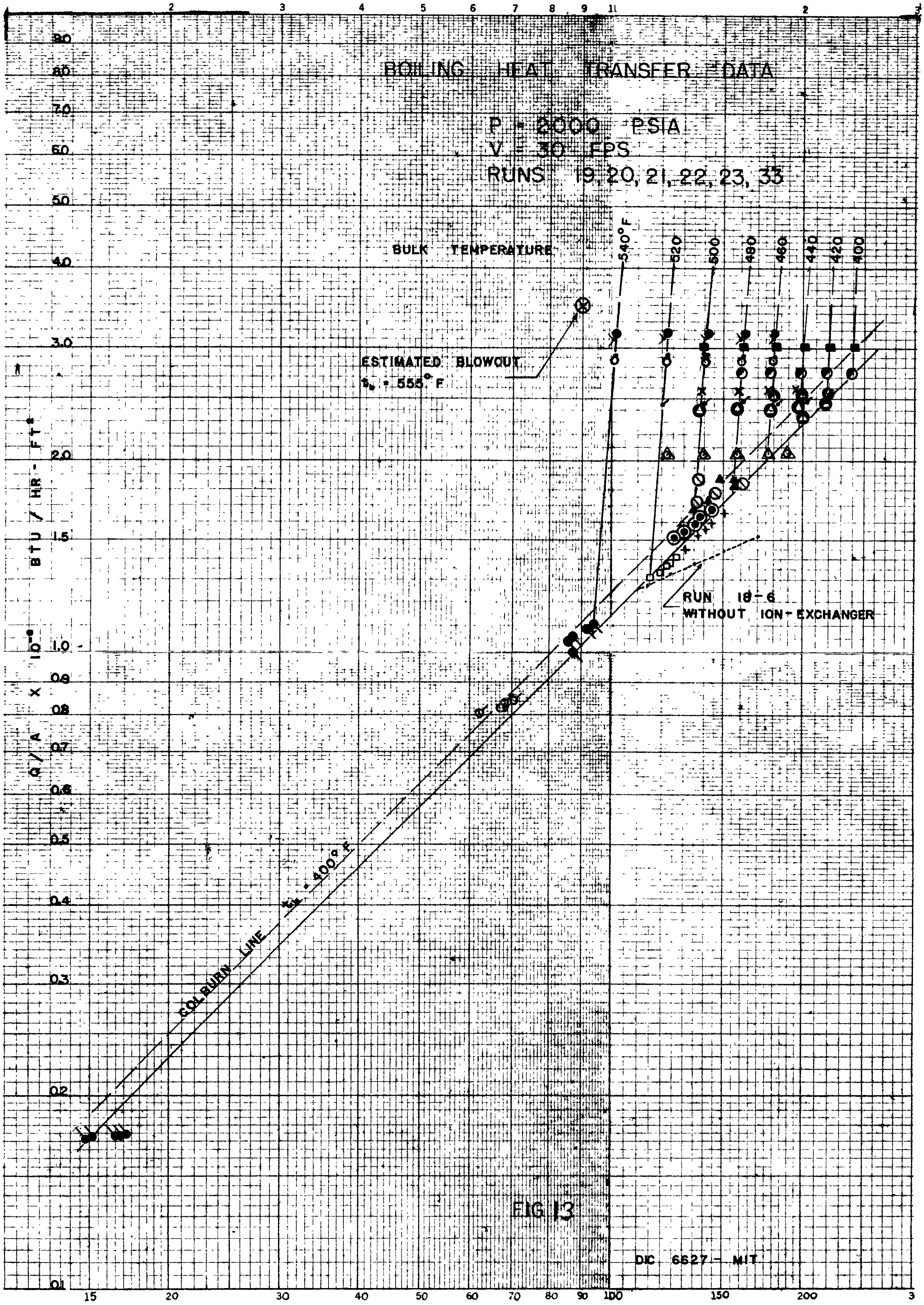

FIG 13

DIC 6627 - MIT

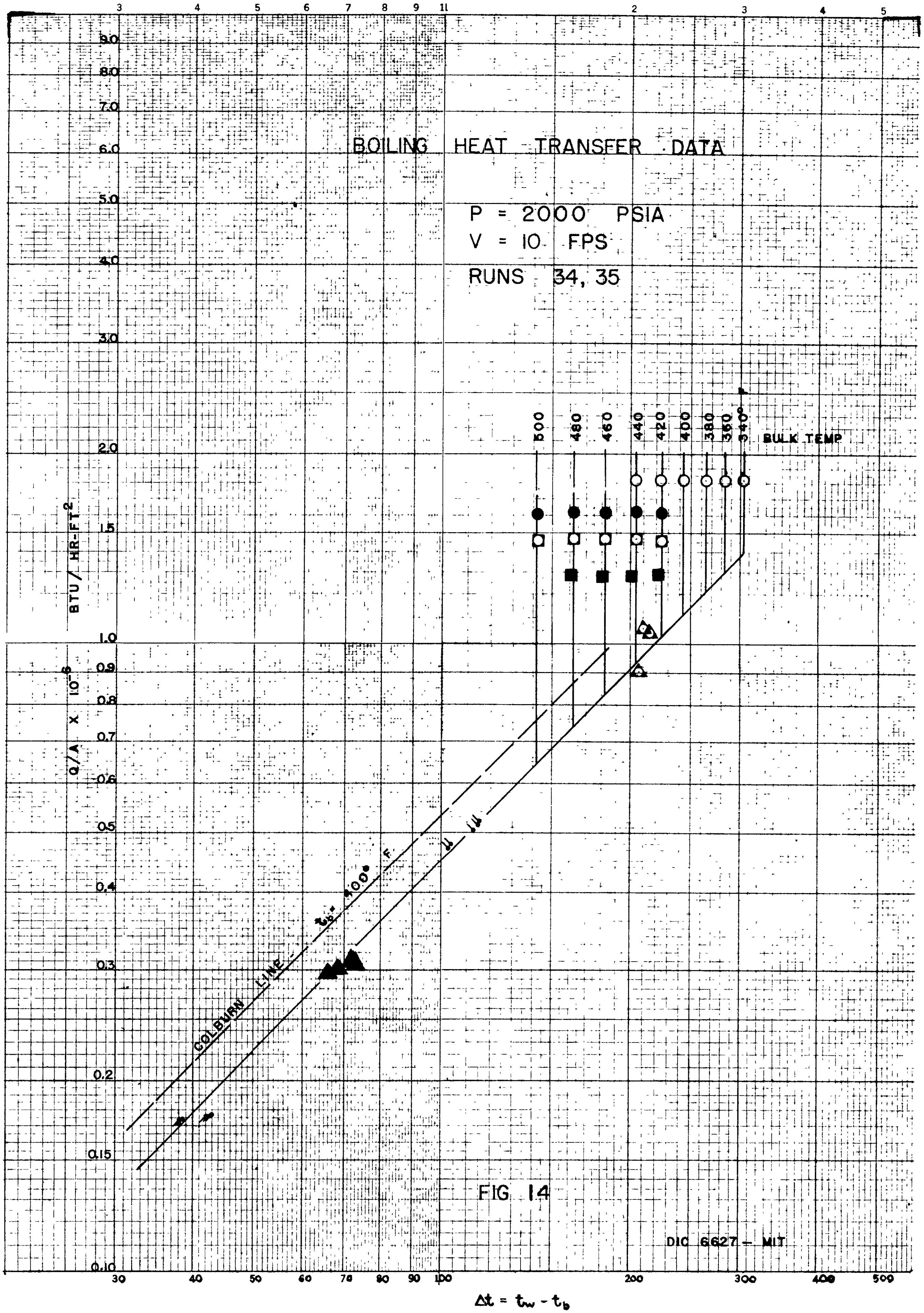

BOILING HEAT TRANSFER DATA

P = 2000 PSIA

V = 10 FPS

RUNS 34, 35

FIG 14

DIC 6627 - MIT

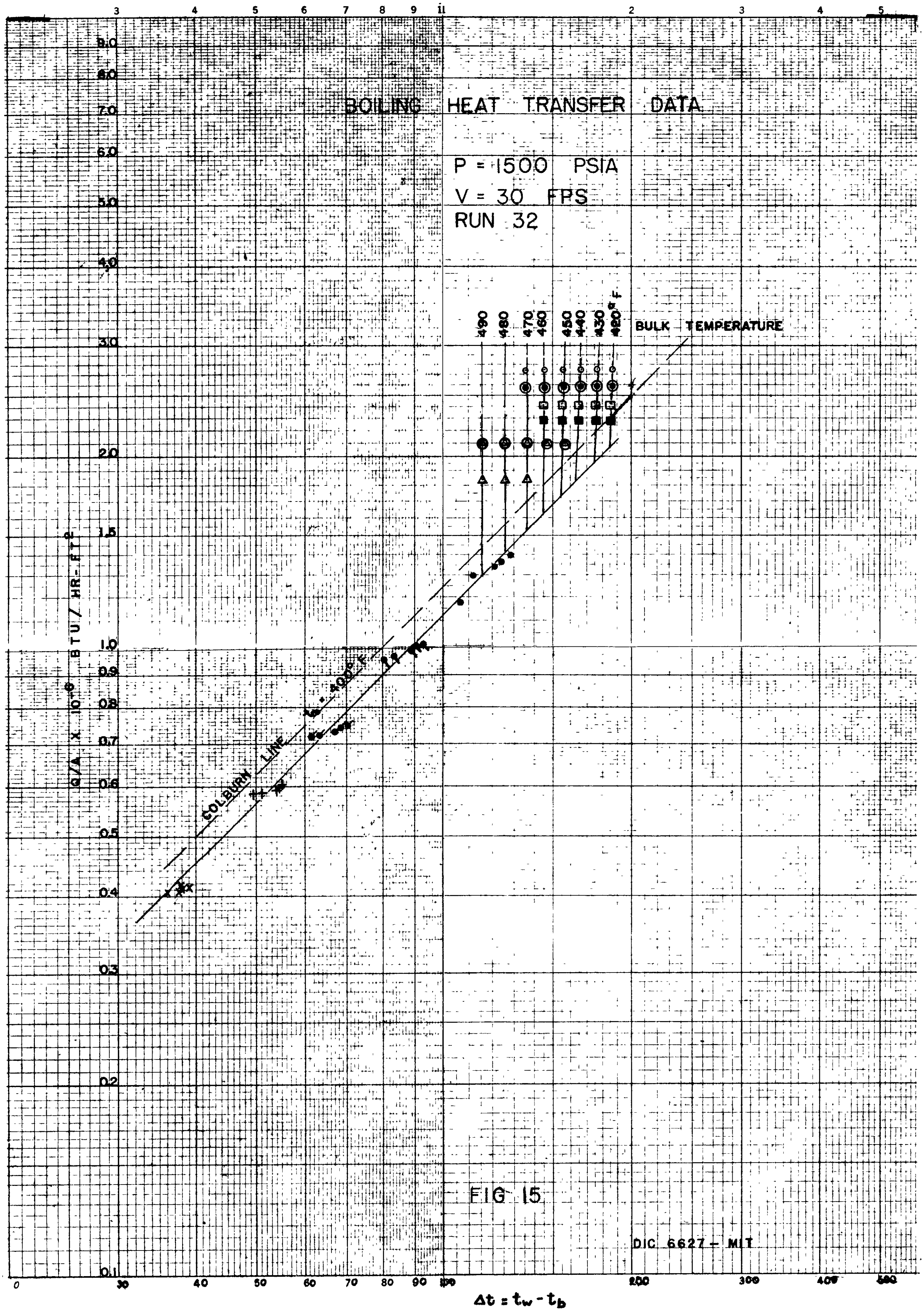
BOILING HEAT TRANSFER DATA
P = 1500 PSIA
V = 30 FPS
RUN 32
BULK TEMPERATURE
490
480
470
460
450
440
430
420° F
COLBURN LINE
$t_b = 400°$ F
$Q/A \times 10^{-6}$ BTU / HR-FT^2
$\Delta t = t_w - t_b$
9.0
8.0
7.0
6.0
5.0
4.0
3.0
2.0
1.5
1.0
0.9
0.8
0.7
0.6
0.5
0.4
0.3
0.2
0.1
30
40
50
60
70
80
90
100
200
300
400
500
DIC 6627 - MIT

FIG 15

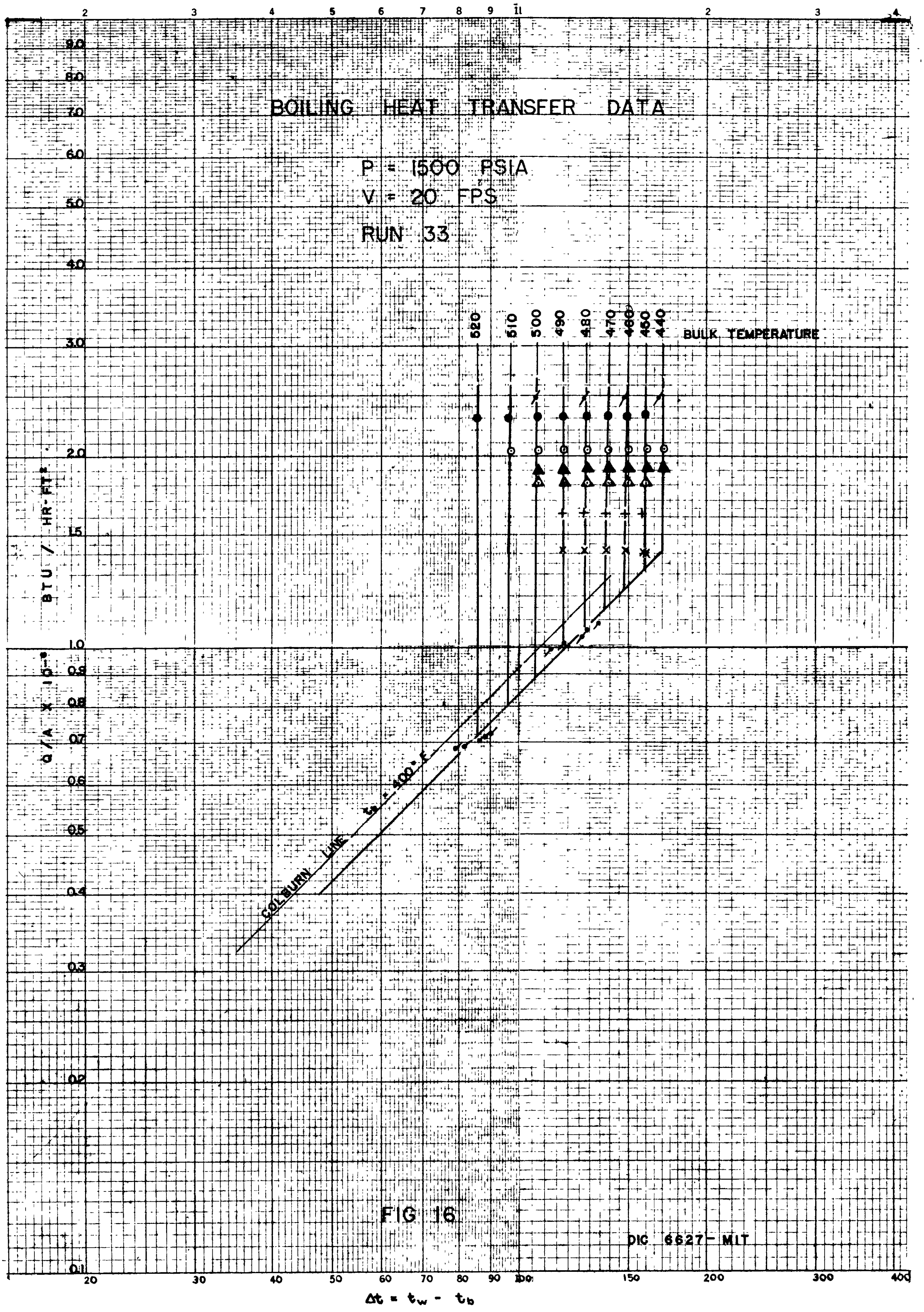
BOILING HEAT TRANSFER DATA
P = 1500 PSIA
V = 20 FPS
RUN 33
520
510
500
490
480
470
460
450
440
BULK TEMPERATURE
COLBURN LINE
t_b = 400° F
Q/A X 10^{-6} BTU / HR-FT²
9.0
8.0
7.0
6.0
5.0
4.0
3.0
2.0
1.5
1.0
0.9
0.8
0.7
0.6
0.5
0.4
0.3
0.2
0.1
20
30
40
50
60
70
80
90
100
150
200
300
400
Δt = t_w - t_b
DIC 6627-MIT

FIG 16

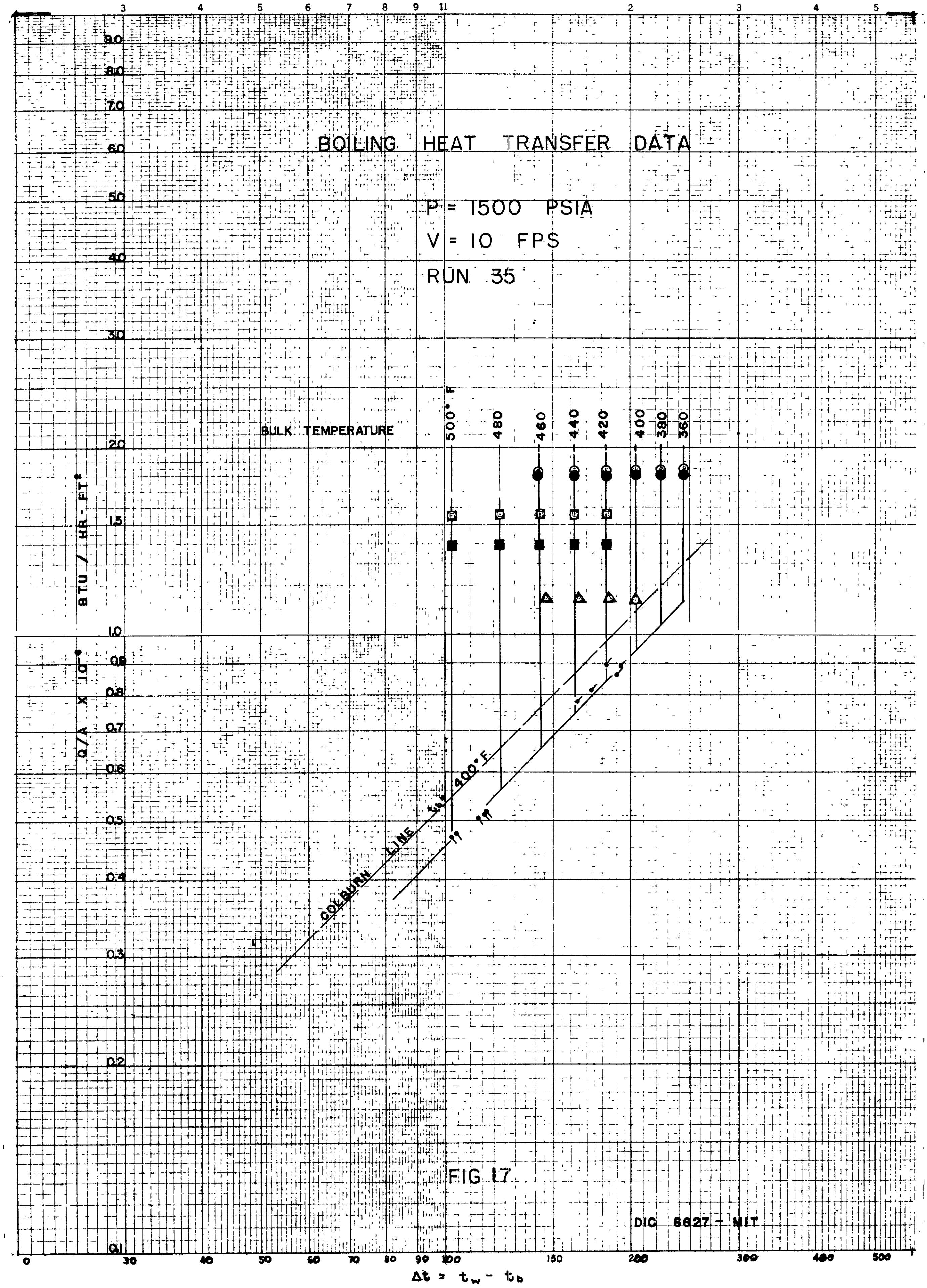

BOILING HEAT TRANSFER DATA

P = 1500 PSIA

V = 10 FPS

RUN 35

FIG 17

Table I Heat Transfer Data Without Surface Boiling

Run No.	Station	Pin psia	Vin f.p.s.	G $\frac{lb_m}{sec/ft^2}$	t_{in} °F	t_{out} °F	Δp "H_2O	Nu_b	Re_f $\times 10^{-3}$	$\frac{c_p \mu_f}{k}$	j $\times 10^{-3}$
19-1	2	2000	29	1570	410	437	152	503	292	.82	1.84
	3							477	300	.77	1.7
	4							482	302	.82	1.7
	5							479	303	.82	1.6
	6							471	307	.80	1.6
20-1	2	2000	29.8	1585	400	436		468	299	.85	1.6
	3							475	305	.785	1.6
	4							458	307	.78	1.6
	5							461	309	.79	1.6
	6							462	311	.795	1.6
20-2	2	2000	29.9	1585	406	454		448	314	.765	1.5
	3							442	323	.76	1.5
	4							444	329	.755	1.4
	5							444	332	.745	1.4
	6							445	339	.73	1.4
21-1	2	2000	29.8	1561	427	482	140	443	329	.75	1.4
	3							443	341	.73	1.4
	4							442	348	.73	1.4
	5							447	353	.715	1.4
	6							446	359	.715	1.3
22-1	2	2000	30.0	1558	446	498	150	481	343	.73	1.5
	3							478	350	.715	1.5
	4							472	353	.715	1.5
	5							483	359	.725	1.5
	6							478	373	.72	1.4
22-2	2	2000	30.0	1548	453	520	155	495	360	.695	1.5
	3										
	4										
	5										
	6										
23-1	2	2000	29.9	1585	383	388	133	441	254	.945	1.7
	3							434	254	.94	1.7
	4							402	355	.94	1.6
	5							397	256	.935	1.5
	6							391	256	.925	1.5

Table I Heat Transfer Data Without Surface Boiling (cont.)

2.

Run No.	Station	Pin psia	Vin f.p.s.	G $\frac{lb_m}{sec/ft^2}$	t_{in} °F	t_{out} °F	ΔP "H_2O	Nu_b	Re_f x 10^{-3}	$\frac{C_p \mu_f}{k}$	j $\times 10^{-3}$
23-2	2	2000	30.0	1562	442	502	130	498	346	.735	1.60
	3							502	356	.71	1.58
	4							506	362	.71	1.57
	5										
	6										
23-3	2	2000	30.0	1570	444	504	130	503	349	.725	1.61
	3							493	356	.72	1.55
	4							477	368	.71	1.45
	5										
	6										
33-11	2	2000	30.0	1618	386	470		453	345	.705	1.48
	3							446	361	.685	1.40
	4										
	5										
	6										
23-4	2	2000	19.9	1051	407	462	64.5	338	210	.785	1.74
	3							335	217	.75	1.70
	4							330	221	.74	1.65
	5							327	228	.73	1.59
	6							324	233	.73	1.55
23-5	2	2000	20.0	1049	426	491	63.5	347	226	.735	1.70
	3							341	233	.715	1.64
	4							332	238	.715	1.56
	5							349	243	.705	1.61
	6										
23-6	2	2000	20.0	1043	438	514	67	350	241	.705	1.63
	3										
	4										
	5										
	6										
30-1	2	2000	20.1	1099	373	414	53.6	313	197	.835	1.69
	3							326	198	.825	1.75
	4							315	202	.815	1.67
	5							314	207	.790	1.64
	6							313	210	.79	1.61

Table I Heat Transfer Data Without Surface Boiling

Run No.	Station	Pin psia	Vin f.p.s.	3 G $\frac{lb_m}{sec/ft^2}$	t_{in} °F	t_{out} °F	ΔP "H_2O	Nu_b	Re_f x 10^{-3}	$\frac{C_p \mu_f}{k}$	ν x10^{3}
30-2	2	2000	20.0	1083	409	467	52.9	315	225	.740	1.55
	3							332	226	.745	1.55
	4							321	236	.72	1.52
	5							321	241	.715	1.49
	6							317	244	.71	1.46
31-1	2	2000	20.1	1132	327	358	57.2	311	170	.96	1.86
	3							322	173	.935	1.91
	4							308	178	.916	1.78
	5							308	180	.90	1.77
	6							304	181	.89	1.74
31-2	2	2000	20.0	1111	350	391	55	311	187	.855	1.75
	3							325	189	.865	1.80
	4							308	195	.835	1.68
	5							315	199	.825	1.69
	6							309	202	.820	1.64
31-3	2	2000	20.1	1100	382	429	54.3	324	203	.805	1.72
	3							334	209	.785	1.73
	4							321	212	.785	1.64
	5							323	217	.765	1.63
	6							319	222	.750	1.58
31-4	2	2000	20.4	1083	408	466	52.2	327	221	.745	1.63
	3							338	226	.745	1.65
	4							325	233	.725	1.55
	5							328	239	.710	1.54
	6							328	244	.720	1.50
31-5	2	2000	20.3	1063	431	504	53	354	239	.710	1.66
	3							347	246	.720	1.57
	4										
	5										
	6										
31-9	2	2000	20.2	1130	340	454	62	331	236	.70	1.58
	3										
	4										
	5										
	6										

Table I Heat Transfer Data Without Surface Boiling (cont.)

Run No.	Station	Pin psia	Vin f.p.s.	G $\frac{lb_m}{sec/ft^2}$	t_{in} °F	t_{out} °F	ΔP "H_2O	Nu_b	Re_f x 10^{-3}	$\frac{C_p \mu_f}{k}$	$j \times 10^3$
34-2	2	2000	10	590	223	252	25	163	59.9	1.38	2.42
	3							164	61.3	1.35	2.42
	4							157	63.8	1.31	2.25
	5							160	64.7	1.28	2.28
	6							161	66.1	1.25	2.26
34-3	2	2000	10	544	371	470	22.9	168	113	.715	1.68
	3							188	118	.690	1.81
	4							198	122	.685	1.86
	5										
	6										
34-4	2	2000	10	560	389	512	22.9				
	3										
	4							275	124	.695	2.60
	5										
	6										
35-1	2	2000	10.0	548	355	370		173	84.1	.945	2.10
	3							169	85.3	.940	2.02
	4							159	86.5	.940	1.88
	5							155	86.8	.930	1.83
	6							157	87.1	.935	1.85
35-2	2	2000	10.0	552	357	405		172	94.8	.855	1.92
	3							177	97.9	.830	1.92
	4							166	100	.830	1.77
	5							169	102	.820	1.77
	6							172	104	.795	1.79
32-1	2	1500	30.0	1727	305	318	117	404	227	1.06	1.71
	3							422	228	1.06	1.78
	4							403	230	1.04	1.78
	5							406	232	1.04	1.77
	6							397	234	1.04	1.72
32-2	2	1500	30.0	1711	314	333	114	439	238	1.01	1.84
	3							432	242	.995	1.79
	4							413	244	.990	1.70
	5							409	245	.990	1.68
	6							412	280	.990	1.68

Table I Heat Transfer Data Without Surface Boiling (cont.)

Run No.	Station	P_{in} psia	V_{in} f.p.s.	G $\frac{lb_m}{sec/ft^2}$	t_{in} °F	t_{out} °F	ΔP "H_2O	Nu_b	Re_f x 10^{-3}	$\frac{C_p\mu_f}{k}$	j $x10^{-3}$
32-3	2	1500	30.0	1665	348	373	110	442	262	.910	[illegible]
	3							433	264	.910	[illegible]
	4							414	268	.910	[illegible]
	5							413	272	.895	1.58
	6							405	276	.875	1.54
32-4	2	1500	30.0	1641	379	412	106	455	291	.850	[illegible]
	3							446	295	.825	[illegible]
	4							426	299	.820	1.55
	5							428	303	.810	1.52
	6							421	312	.795	[illegible]
32-5	2	1500	30.2	1570	423	467	102	439	321	.765	[illegible]
	3							461	327	.745	[illegible]
	4							442	335	.740	[illegible]
	5							441	341	.730	[illegible]
	6							438	349	.715	[illegible]
33-2	2	1500	20.6	1161	323	357	56.2	323	174	.960	[illegible]
	3							317	177	.940	[illegible]
	4							307	182	.910	1.74
	5							305	185	.895	1.71
	6							302	188	.885	1.69
33-3	2	1500	20.2	1090	376	427	52.2	334	201	.820	[illegible]
	3							330	206	.795	1.73
	4							319	211	.770	1.65
	5							320	216	.770	1.62
	6							316	222	.760	1.58
35-3	2	1500	10.0	545	355	404	16.4	177	94	.845	1.99
	3							178	96.5	.835	1.94
	4							169	98.8	.825	1.83
	5							169	100	.810	1.82
	6							171	103	.790	1.79
35-4	2	1500	10.0	549	357	439	16.4	182	105	.785	1.89
	3							181	109	.765	1.82
	4							175	114	.730	1.71
	5										
	6										

TABLE II

HEAT TRANSFER DATA WITH SURFACE BOILING

Run No.	Station	G lb $lb/sec.ft^2$	p psia	Vin ft/sec.	tw °F	τ °F	Tx °F	Δt subcool °F	q/A $Btu/hr.ft^2$	Tx avg.
21-2	2	1585	2000	30.1	641.5	445	5.7	191	2.4×10^6	6.5
	3				642.5	457	6.7	179	2.4×10^6	
	4				643.5	469	7.7	167	2.41×10^6	
	5				641.5	481	5.7	155	2.40×10^6	
	6				642.5	493	6.7	143	2.40×10^6	
21-3	2	1561	2000	29.9	641	448	5.2	188	2.57×10^6	6.6
	3				642	461	6.2	175	2.58×10^6	
	4				643.5	473.5	7.7	152.5	2.59×10^6	
	5				642	486	6.2	150	2.58×10^6	
	6				643.5	499	7.7	137	2.59×10^6	
22-2	3	1548	2000	30.0	640	476.5	4.2	159.5	2.04×10^6	5.45
	4				642	486.5	6.2	149.5	2.055×10^6	
	5				641	496.5	5.2	139.5	2.054×10^6	
	6				642	506.5	6.2	129.5	2.055×10^6	
22-3	2	1553	2000	30.0	642	468.5	6.2	167.5	2.44×10^6	7.8
	3				643	480	7.2	156	2.44×10^6	
	4				645	492	9.2	144	2.44×10^6	
	5				644	504	8.2	132	2.44×10^6	
	6				644	516	8.2	120	2.44×10^6	
22-4	2	1553	2000	30.0	644	473	8.2	163	2.89×10^6	9.8
	3				645	487	9.2	149	2.90×10^6	
	4				647	501	11.2	135	2.90×10^6	
	5				646	515	10.2	121	2.90×10^6	
	6				646	529	10.2	107	2.90×10^6	
22-5	2	1553	2000	30.0	646	471.5	10.2	164.5	2.895×10^6	10.8
	3				646	485.5	10.2	150.5	2.895×10^6	
	4				648	499.5	12.2	136.5	2.91×10^6	
	5				646	513.5	10.2	122.5	2.895×10^6	
	6				647	527.5	11.2	108.5	2.91×10^6	
22-6	2	1548	2000	30.0	647	473	11.2	163	3.15×10^6	11.4
	3				647	489	11.2	147	3.15×10^6	
	4				649	505	13.2	131	3.16×10^6	
	5				647	520	11.2	116	3.15×10^6	
	6				646	534	10.2	102	3.15×10^6	
22-7	2	1548	2000	30.0	646.5	471	10.7	165	3.12×10^6	10.1
	3				646.5	486.5	10.7	149.5	3.12×10^6	
	4				646.5	501.5	10.7	134.5	3.12×10^6	
	5				645.5	516.5	9.7	119.5	3.12×10^6	
	6				644.5	531.5	8.7	104.5	3.11×10^6	

TABLE II

HEAT TRANSFER DATA WITH SURFACE BOILING

Run No.	Station	G lb lb/sec.ft^2	p psia	Vin ft/sec.	tw °F	τ °F	Tx °F	Δt subcool °F	q/A Btu/hr.ft^2	Tx avg.
23-2	5	1562	2000	30.0	640.5	481	4.7	155	1.86×10^6	4.7
	6				640.5	489.5	4.7	146.5	1.86×10^6	
23-3	5	1570	2000	30.0	641	483	5.2	153	1.86×10^6	4.2
	6				639	491.5	3.2	144.5	1.86×10^6	
33-11	4	1618	2000	30.0	643.5	428	7.7	208	2.53×10^6	7.33
	5				643.5	440.5	7.7	195.5	2.53×10^6	
	6				642.5	453	6.7	183	2.53×10^6	
33-12	2	1610	2000	30.0	642	416.5	6.2	219.5	2.75×10^6	7.0
	3				643.5	430	7.7	206	2.76×10^6	
	4				644	443.5	8.2	192.5	2.76×10^6	
	5				643	457	7.2	179	2.76×10^6	
	6				641.5	470.5	5.7	165.5	2.75×10^6	
33-13	2	1602	2000	29.7	644.5	423	8.7	213	3.00×10^6	8.1
	3				644.5	438	8.7	198	3.00×10^6	
	4				644.5	453	8.7	183	3.00×10^6	
	5				643.5	468	7.7	168	3.00×10^6	
	6				642.5	483	6.7	153	2.99×10^6	
23-6	3	1043	2000	20.0	639	465	3.2	171	1.57×10^6	5.7
	4				642	476	6.2	160	1.58×10^6	6.5
	5				643	487	7.2	149	1.58×10^6	
	6				642	499	6.2	137	1.58×10^6	
23-5	6	1049	2000	20.0	639.5	478	3.7	158	1.37×10^6	3.7
30-3	2	1051	2000	20.1	642.5	454	6.7	182	1.78×10^6	7.9
	3				643.5	467	7.7	169	1.78×10^6	
	4				644.5	479	8.7	157	1.79×10^6	
	5				644.5	492	8.7	144	1.79×10^6	
	6				643.5	505	7.7	131	1.78×10^6	
30-4	2	1052	2000	20.1	643	460	7.2	176	2.03×10^6	8.3
	3				643.5	475	7.7	161	2.03×10^6	
	4				645	489	9.2	147	2.03×10^6	
	5				645	504	9.2	132	2.03×10^6	
	6				644	519	8.2	117	2.03×10^6	
30-5	2	1059	2000	20.1	644.5	450	8.7	186	2.21×10^6	9.6
	3				645	466	9.2	170	2.20×10^6	
	4				646.5	482	10.7	154	2.23×10^6	
	5				646	498	10.2	138	2.23×10^6	
	6				645	514	9.2	122	2.23×10^6	

TABLE II

HEAT TRANSFER DATA WITH SURFACE BOILING

Run No.	Station	G lb $lb/sec.ft^2$	p psia	Vin ft/sec.	tw °F	τ °F	Tx °F	Δt subcool °F	q/A $Btu/hr.ft^2$	Tx avg.
30-6	2	1059	2000	20.1	643	445	7.2	191	2.02 x 10^6	7.8
	3				644	459	8.2	177	2.02 x 10^6	
	4				644	474	8.2	162	2.03 x 10^6	
	5				644	488	8.2	148	2.03 x 10^6	
	6				643	503	7.2	133	2.03 x 10^6	
31-5	4	1063	2000	20.3	643	468	7.2	168	1.54 x 10^6	7.2
	5				643	479	7.2	157	1.54 x 10^6	
	6				643	489	7.2	147	1.54 x 10^6	
31-6	2	1060	2000	20.3	642.5	452	6.7	184	1.74 x 10^6	7.9
	3				643.5	464	7.7	172	1.74 x 10^6	
	4				644.5	477	8.7	159	1.74 x 10^6	
	5				644.5	489	8.7	147	1.74 x 10^6	
	6				643.5	502	7.7	134	1.74 x 10^6	
31-7	2	1057	2000	20.1	643.5	440	7.7	196	1.91 x 10^6	8.3
	3				644.5	454	8.7	182	1.92 x 10^6	
	4				644.5	468	8.7	168	1.92 x 10^6	
	5				644.5	482	8.7	154	1.92 x 10^6	
	6				643.5	495	7.7	141	1.91 x 10^6	
31-8	2	1057	2000	20.1	644.5	204.5	8.7	196	2.09 x 10^6	8.9
	3				645.5	190.5	9.7	181	2.11 x 10^6	
	4				645.5	175.5	9.7	166	2.11 x 10^6	
	5				644.5	159.5	8.7	151	2.09 x 10^6	
	6				643.5	143.5	7.7	136	2.07 x 10^6	
31-9	3	1130	2000	20.2	645	380	9.2	256	2.34 x 10^6	9.95
	4				647	397	11.2	239	2.34 x 10^6	
	5				646	413	10.2	213	2.34 x 10^6	
	6				645	430	9.2	206	2.34 x 10^6	
31-10	2	1118	2000	20.1	643.5	365	7.7	271	2.53 x 10^6	8.9
	3				645.5	384	9.7	252	2.54 x 10^6	
	4				646.5	403	10.7	234	2.54 x 10^6	
	5				644.5	421	8.7	216	2.54 x 10^6	
	6				643.5	439	7.7	197	2.53 x 10^6	
34-3	5	544	2000	10.0	639.5	434	3.7	200	1.08 x 10^6	4.7
	6				641.5	450	5.7	185	1.08 x 10^6	
34-4	2	560	2000	10.0	642	413.5	6.2	222.5	1.29 x 10^6	(4.8)
	3				638	431.5	2.2	204.5	1.28 x 10^6	(5.4)
	5				641	467.5	5.2	168.5	1.29 x 10^6	
	6				641.5	485.5	5.7	150.5	1.29 x 10^6	

TABLE II

HEAT TRANSFER DATA WITH SURFACE BOILING

Run No.	Station	G lb lb/sec.ft^2	p psia	Vin ft/sec.	tw °F	$\mathcal{T}$ °F	Tx °F	Δt subcool °F	q/A Btu/hr.ft^2	Tx avg.
34-5	2	541	2000	10.0	641.5	415	5.7	221	1.46 x 10^6	7.1
	3				643	436	7.2	200	1.47 x 10^6	
	4				644.5	457	8.7	179	1.47 x 10^6	
	5				643.5	478	7.7	158	1.47 x 10^6	
	6				642	499	6.2	137	1.46 x 10^6	
34-6	2	545	2000	10.0	642.5	407	6.7	229	1.61 x 10^6	7.5
	3				643.5	430	7.7	206	1.62 x 10^6	
	4				645	453	9.2	183	1.62 x 10^6	
	5				643.5	476	7.7	160	1.62 x 10^6	
	6				642	499	6.2	137	1.61 x 10^6	
34-7	2	550	2000	9.8	643	346	7.2	290	1.82 x 10^6	7.8
	3				644	374	8.2	262	1.82 x 10^6	
	4				645	402	9.2	234	1.82 x 10^6	
	5				643.5	428	7.7	212	1.82 x 10^6	
	6				642.5	454	6.7	182	1.81 x 10^6	
32-6	2	1552	1500	29.9	604	451.5	7.8	144.5	1.82 x 10^6	11.5 (12.4)
	3				607	460.5	10.8	135.5	1.84 x 10^6	
	4				610	469.5	13.8	127.5	1.85 x 10^6	
	5				609	478.5	12.8	118.5	1.84 x 10^6	
	6				608.5	487.5	12.3	108.5	1.84 x 10^6	
32-7	2	1552	1500	29.9	608.5	445.5	12.8	150.5	2.09 x 10^6	13.5
	3				610	456	13.8	140	2.10 x 10^6	
	4				611	466.5	14.8	129.5	2.11 x 10^6	
	5				609.5	477	13.3	119	2.10 x 10^6	
	6				609	487.5	12.8	108.5	2.10 x 10^6	
32-8	2	1618	1500	30.0	600.5	406	4.3	190	2.25 x 10^6	10.7 (12.3)
	3				607	417.5	10.8	178.5	2.28 x 10^6	
	4				609.5	429	13.3	167	2.29 x 10^6	
	5				609	440.5	12.8	155.5	2.29 x 10^6	
	6				608.5	452	12.3	144	2.29 x 10^6	
32-9	2	1610	1500	29.8	607	413.5	10.8	182.5	2.40 x 10^6	12.6
	3				609.5	425.5	13.3	170.5	2.42 x 10^6	
	4				610	437.5	13.8	159.5	2.42 x 10^6	
	5				609	449.5	12.8	146.5	2.42 x 10^6	
	6				608.5	461.5	12.3	134.5	2.41 x 10^6	
32-10	2	1610	1500	29.8	610	414.5	13.8	181.5	2.58 x 10^6	14.1
	3				610.5	427.5	14.3	169.5	2.59 x 10^6	
	4				610.5	440.5	14.3	155.5	2.59 x 10^6	
	5				610.5	453.5	14.3	142.5	2.59 x 10^6	
	6				610	466.5	13.8	129.5	2.58 x 10^6	

TABLE II

HEAT TRANSFER DATA WITH SURFACE BOILING

Run No.	Station	G lb lb/sec.ft^2	p psia	Vin ft/sec.	tw °F	τ °F	Tx °F	Δt subcool °F	q/A Btu/hr.ft^2	Tx avg.
32-11	2	1593	1500	29.7	611	414.5	14.8	181.5	2.75 x 10^6	14.5
	3				611	428	14.8	168	2.75 x 10^6	
	4				611	442	14.8	154	2.75 x 10^6	
	5				610.5	456	14.3	140	2.75 x 10^6	
	6				609.5	469.5	13.3	126.5	2.74 x 10^6	
33-4	2	1051	1500	20.1	606	444	9.8	152	1.40 x 10^6	12.4
	3				608.5	454	12.3	142	1.41 x 10^6	
	4				610	464	13.8	132	1.42 x 10^6	
	5				609.5	474	13.3	122	1.42 x 10^6	
	6				609	484	12.8	112	1.42 x 10^6	
33-5	2	1059	1500	20.1	609.5	441	13.3	155	1.62 x 10^6	13.8
	3				610.5	452.5	14.3	143.5	1.62 x 10^6	
	4				610.5	464	14.3	132	1.62 x 10^6	
	5				610	475.5	13.8	120.5	1.62 x 10^6	
	6				609.5	487	13.3	109	1.62 x 10^6	
33-6	2	1051	1500	20.0	610.5	443.5	14.3	152.5	1.81 x 10^6	14.4
	3				611.5	457	15.3	139	1.82 x 10^6	
	4				611	470	14.8	126	1.81 x 10^6	
	5				610.5	483.5	14.3	112.5	1.81 x 10^6	
	6				609.5	496.5	13.3	99.5	1.81 x 10^6	
33-7	2	1051	1500	20.0	611.5	441	15.3	155	1.91 x 10^6	15.2
	3				612	455	15.8	141	1.91 x 10^6	
	4				611.5	469	15.3	127	1.91 x 10^6	
	5				610.5	483	14.3	113	1.90 x 10^6	
	6				609.5	497	13.3	99	1.90 x 10^6	
33-8	2	1050	1500	20.0	613	445	16.8	151	2.06 x 10^6	15.2
	3				612.5	461	16.3	135	2.06 x 10^6	
	4				611.5	476	15.3	120	2.05 x 10^6	
	5				610.5	491	14.3	105	2.05 x 10^6	
	6				609.5	506	13.3	90	2.04 x 10^6	
33-9	2	1051	1500	20.1	612	449	15.8	147	2.32 x 10^6	14.8
	3				612	465.5	15.8	130.5	2.31 x 10^6	
	4				611	482	14.8	114	2.31 x 10^6	
	5				610.5	498.5	14.3	97.5	2.31 x 10^6	
	6				609.5	515	13.3	81	2.30 x 10^6	
33-10	2	1057	1500	20.1	611.5	437	15.3	159	2.49 x 10^6	14.4
	3				611.5	455	15.3	141	2.49 x 10^6	
	4				610.5	473	14.3	123	2.48 x 10^6	
	5				610.0	491	13.8	105	2.48 x 10^6	
	6				609.5	509	13.3	97	2.48 x 10^6	

TABLE II

HEAT TRANSFER DATA WITH SURFACE BOILING

Run No.	Station	G lb lb/sec.ft^2	p psia	Vin ft/sec.	tw °F	τ °F	Tx °F	Δt subcool °F	q/A Btu/hr.ft^2	Tx avg.
35-4	5	549	1500	10.02	603.5	410	7.3	186	.896 x 10^6	8.8
	6				606.5	422	10.3	174	.896 x 10^6	
35-5	2	543	1500	10.02	605	398.5	8.8	197.5	1.12 x 10^6	10.6
	3				606	415	9.8	181	1.13 x 10^6	
	4				608	431.5	11.8	164.5	1.14 x 10^6	
	5				607.5	448	11.3	148	1.14 x 10^6	
	6				607.5	464.5	11.3	131.5	1.14 x 10^6	
35-6	2	541	1500	10.03	604	422.5	7.8	173.5	1.39 x 10^6	8.1
	3				604	442	7.8	154	1.39 x 10^6	
	4				605	461.5	8.8	134.5	1.39 x 10^6	
	5				604.5	481	8.3	115	1.39 x 10^6	
	6				604	500.5	7.8	95.5	1.39 x 10^6	
35-7	2	541	1500	10.01	604.5	415	8.3	181	1.56 x 10^6	8.0
	3				604.5	437	8.3	159	1.56 x 10^6	
	4				604.5	459	8.3	137	1.56 x 10^6	
	5				604.5	481	8.3	115	1.56 x 10^6	
	6				603	503	6.8	93	1.55 x 10^6	
35-8	2	559	1500	9.9	606.5	344	10.3	252	1.81 x 10^6	9.7
	3				606.5	370	10.3	226	1.81 x 10^6	
	4				606.5	396	10.3	200	1.81 x 10^6	
	5				605.5	422	9.3	174	1.80 x 10^6	
	6				604.5	448	8.3	148	1.80 x 10^6	
35-9	2	556	1500	9.9	607	355	10.8	241	1.85 x 10^6	9.4
	3				606.5	382	10.3	234	1.84 x 10^6	
	4				606.5	409	10.3	187	1.84 x 10^6	
	5				604.5	436	8.3	160	1.84 x 10^6	
	6				603.5	463	7.3	133	1.83 x 10^6	

Table III PRESSURE DROP WITHOUT SURFACE BOILING

Run No.	G	V_{in}	$T_{w, avg}$	τ_{in}	τ_{out}	μ_b/μ_w	$\Delta P_{f,m}$	f_f	$f_{f,m}$	$f_{isotherm}$	$N_{Re,b}$
	$\frac{lb._m}{sec.ft^2}$	$\frac{ft.}{sec.}$	°F	°F	°F	at τ_{avg}	"H_2O	$x10^5$	$x\ 10^5$	$x\ 10^5$	at τ_{avg}
					Pressure 2000 psia						
30-1	1098	20.1	492	373	414	1.275	54.8	360	388	405	178,500
-2	1081	20.0	583	409	467	1.34	54.4	345	392	395	198,000
31-1	1132	20.1	420	327	358	1.25	58.1	383	401	415	157,000
-2	1114	20.0	473	350	391	1.31	56.0	365	392	410	169,400
-3	1098	20.1	522	382	429	1.305	55.6	350	382	400	185,500
-4	1081	20.4	581	408	466	1.35	53.7	328	373	396	197,000
					Pressure 1500 psia						
32-1	1728	30.0	349	305	318	1.13	117.3	355	360	388	217,200
-2	1712	30.0	378	314	333	1.17	115.0	343	354	385	226,000
-3	1665	30.0	428	348	373	1.185	111.0	330	346	378	248,500
-4	1640	30.0	486	379	412	1.26	107.2	320	342	372	268,500
-5	1570	30.2	566	423	367	1.31	103.1	295	333	365	293,000
33-2	1162	20.6	426	323	357	1.29	57.4	355	375	412	161,200
-3	1090	20.2	527	376	427	1.33	53.5	338	374	400	184,000

Table IV PRESSURE DROP WITH SURFACE BOILING

Run No.	p	V_{in}	G	$q/A \times 10^{-6}$	$t_{w,avg}$	τ_{in}	τ_{out}	$t_{sat\ avg}$	Δp_{fm}	Δp_f
	psia	ft/sec	$lb_m/sec.ft^2$	$Btu/hr.ft^2$	F	F	F	F	"H_2O	"H_2O
33-11	2000	30.0	1618	2.53	643	386	470	208	111.1	90.1
12		30.0	1610	2.76	643	398	491	191	115.8	90.3
13		29.7	1602	3.00	644	403	503	183	123.1	94.8
30- 3	2000	20.1	1051	1.78	644	436	523	156	57.0	44.7
4		20.1	1052	2.03	644	440	539	146	63.8	49.5
5		20.1	1059	2.23	645	428	537	153	65.6	50.3
6		20.1	1059	2.20	644	424	523	162	65.7	51.9
31- 5		20.3	1063	1.54	643	431	504	168	53.5	43.7
6		20.3	1060	1.74	644	435	519	159	57.7	46.1
7		20.1	1057	1.92	644	421	514	168	62.6	50.3
8		20.1	1057	2.10	645	420	520	166	62.7	49.5
9		20.2	1130	2.34	646	340	454	239	59.9	47.8
10		20.1	1118	2.54	645	340	464	234	60.5	47.2
34- 5	2000	10.0	541	1.47	643	387	527	179	26.8	21.9
6		10.0	545	1.62	643	376	531	182	29.6	24.3
7		9.8	550	1.82	644	309	487	242	31.1	25.3
32- 6	1500	29.9	1552	1.84	608	439	500	107	107.5	89.5
7		29.9	1552	2.10	609	431	501	130	118.1	97.5
8		30.0	1618	2.29	608	390	468	167	115.4	95.1
9		29.8	1610	2.42	609	397	478	158	117.3	96.1
10		29.8	1610	2.59	610	397	484	156	123.0	99.5
11		29.7	1593	2.75	611	396	489	154	126.0	101.0
33 -4	1500	20.1	1051	1.42	609	430	499	132	55.6	46.4
5		20.1	1059	1.62	610	425	504	131	61.2	52.6
6		20.0	1051	1.81	610	426	515	125	67.7	55.2
7		20.0	1051	1.91	611	422	517	126	72.0	59.2
8		20.0	1050	2.05	611	426	527	119	74.3	60.3
9		20.1	1051	2.31	611	427	539	113	81.8	54.0
10		20.1	1057	2.59	611	413	534	122	84.6	66.7
35- 5	1500	10.0	543	1.14	607	376	487	164	22.6	19.3
6		10.0	541	1.39	604	396	528	134	26.7	22.2
7		10.0	541	1.56	604	385	534	136	27.7	22.5
8		9.9	559	1.81	606	309	485	199	27.9	21.9
9		9.9	556	1.84	606	319	499	187	29.0	24.0

ONR:438:JMC:bs
NR-035-267
Ser 8466

DISTRIBUTION LIST

April 27, 1950

Chief of Naval Research
Department of the Navy
Washington 25, D. C.
Attn: Code 438 (2)

Director, Naval Research Laboratory
Washington 25, D. C.
Attn: Tech. Info. Officer (9)
Technical Library (1)
Mechanics Division (2)

Commanding Officer
Office of Naval Research
Branch Office
495 Summer Street
Boston 10, Mass. (2)

Commanding Officer
Office of Naval Research
Branch Office
346 Broadway
New York 13, N. Y. (1)

Commanding Officer
Office of Naval Research
Branch Office
844 N. Rush Street
Chicago 11, Illinois (1)

Commanding Officer
Office of Naval Research
Branch Office
801 Donahue Street
San Francisco 24, Calif. (1)

Commanding Officer
Office of Naval Research
Branch Office
1030 Green Street
Pasadena, Calif. (1)

Contract Administrator, SE Area
Office of Naval Research
Department of the Navy
Washington 25, D. C.
Attn: Mr. R. F. Lynch (1)

Assistant Naval Attache for Research
London
U. S. Navy
FPO 100
New York, N. Y. (5)

Library of Congress
Washington 25, D. C.
Attn: Navy Research Section (2)

Research and Development Board
Department of Defense
Pentagon Building
Washington 25, D. C.
Attn: Library (Code 3D-1075) (1)

Chief of Bureau of Aeronautics
Navy Department
Washington 25, D. C.
Attn: TD-41, Technical Library (1)
PP-22 (1)

Chief of Bureau of Ordnance
Navy Department
Washington 25, D. C.
Attn: Ad-3, Technical Library (2)

Chief of Bureau of Ships
Navy Department
Washington 25, D. C.
Attn: Director of Research (2)
Code 390 (3)
Code 646 (2)
Code 432 (1)

Superintendent
Post Graduate School
U. S. Naval Academy
Annapolis, Maryland (1)

Naval Ordnance Laboratory
White Oak, Maryland
RFD 1, Silver Spring, Maryland
Attn: Mechanics Division (1)

Naval Ordnance Test Station
Inyokern, California
Attn: Scientific Officer (1)

Director,
Naval Engineering Experiment Station
Annapolis, Maryland (2)

Chief of Staff
Department of the Army
The Pentagon
Washington 25, D. C.
Attn: Director of Research
and Development (1)

Distribution List (cont.)

Office of Chief of Ordnance
Research and Development Service
Department of the Army
The Pentagon
Washington 25, D. C.
Attn: ORDTB (1)

Commanding General
U. S. Air Forces
The Pentagon
Washington 25, D. C.
Attn: Research & Development Div. (1)

Office of Air Research
Wright-Patterson Air Force Base
Dayton, Ohio
Attn: Chief, Applied Mechanics Group (1)

U. S. Atomic Energy Commission
Division of Research
Washington, D. C. (1)

Argonne National Laboratory
P. O. Box 5207
Chicago 80, Illinois
Attn: W. H. Jens (25)

U. S. Coast Guard
1300 E Street, N. W.
Washington, D. C.
Attn: Chief, Testing and Development Division (1)

National Advisory Committee for Aeronautics
Cleveland Municipal Airport
Cleveland, Ohio
Attn: J. H. Collins, Jr. (2)

Dr. William Sibbitt
Purdue Research Foundation
Purdue University
Lafayette, Indiana (1)

Professor E. D. Kane
University of California
Berkeley, California (1)

Dr. J. V. Foa
Cornell Aeronautical Laboratory
Buffalo, New York (1)

Professor John W. Hazen
Engineering Research Division
University of California
Los Angeles 24, California (1)

Professor W. H. McAdams
Department of Chemical Engineering
Massachusetts Institute of Technology
Cambridge 39, Massachusetts (1)

Professor A. L. London
Department of Mechanical Engineering
Stanford University
Stanford, California (1)

Professor Warren Rohsenow
Mechanical Engineering Department
Massachusetts Institute of Technology
Cambridge 39, Massachusetts (15)

Lt. Cdr. E. P. Wilkinson
c/o U. S. Atomic Energy Commission
P. O. Box 1105
Pittsburgh 30, Pa. (2)

Mr. R. A. Bowman
Westinghouse Electric Co.
Atomic Power Division
P. O. Box 1468
Pittsburgh, Pa. (1)

Dean L. M. K. Boelter
Dept. of Engineering
University of California
Los Angeles, California (1)

Professor J. H. Keenan
Dept. of Mechanical Engr.
Mass. Inst. of Technology
Cambridge 39, Massachusetts (1)

Professor J. N. Addoms
Dept. of Chemical Engr.
Mass. Inst. of Technology
Cambridge 39, Massachusetts (1)

Dean W. J. Wohlenberg
School of Engineering
Yale University
New Haven, Conn. (1)

Mr. E. E. Ross
Room 20-E-226
Mass. Inst. of Technology
Cambridge 39, Mass. (1)

Distribution Also to Include the Following

Mr. Robert Bromberg
Engineering Research
Department of Engineering
University of California
Los Angeles 24, California (1)

Commandor E. B. Roth
Office of Chicago Directed Operations
U. S. Atomic Energy Commission
P. O. Box 4160 A
Chicago 80, Illinois (1)

Mr. H. Etherington, Director
Naval Reactor Division
Argonne National Laboratory
P. O. Box 5207
Chicago 80, Illinois (4)

Mr. Ben Pinkel
National Advisory Committee
for Aeronautics
Lewis Flight Propulsion Laboratory
Municipal Airport
Cleveland, Ohio (2)

Reference Services Branch
Technical Information Service
U. S. Atomic Energy Commission
Oak Ridge, Tennessee
Attn: I. A. Warheit, Chief (4)

Mr. E. P. Kranzfelder
Babcock & Wilcox Company
Research & Development Dept.
Alliance, Ohio (2)

Dr. George A. Hawkins
Purdue University
Lafayette, Indiana (1)

Mr. Fred Gunther
Jet Propulsion Laboratory
California Institute of Technology
Pasadena, California (1)

Mr. H. S. Isbin
Hanford Works
P. O. Box 550
Richland, Washington (1)

Mr. Gilbert L. Campbell
Library
Los Alamos Scientific Laboratory
P. O. Box 1663
Los Alamos, New Mexico (3)

J. C. Morris
Chief Librarian
Oak Ridge National Laboratory
P. O. Box P
Oak Ridge, Tennessee (3)

Miss Hazel Hutcheson, Librarian
Westinghouse Electric Corporation
Atomic Power Division
P. O. Box 1468
Pittsburgh 30, Pennsylvania (3)

Mr. Joel V. Levy
Department of the Navy
Bureau of Ships
Washington 25, D. C. (1)

Mr. Spencer C. Stanford
Library
Brookhaven National Laboratory
Upton, Long Island, New York (3)

Mr. W. E. Shoupp
Director of Research
Westinghouse Electric Corporation
Atomic Power Division
P. O. Box 1468
Pittsburgh 30, Pennsylvania (1)

Library
Fairchild Engine & Airplane Corp.
NEPA Division
P. O. Box 415
Oak Ridge, Tennessee (3)

Dr. R. M. Lyon
Technical Division
Oak Ridge National Laboratory
Oak Ridge, Tennessee (1)

Mr. W. K. Woods
3703 Building
General Electric Company
Richland, Washington (1)

Mr. N. F. Lansing
Oak Ridge National Laboratory
P. O. Box P
Oak Ridge, Tennessee (1)

Mr. Frederick T. Hobbs
Technical Cooperation Branch
Division of Research
AEC
Washington, D. C. (1)

Mr. H. V. Lichtenberger
Argonne National Laboratory
P. O. Box 5207
Chicago 80, Illinois (1)

H. D. Young
Information Division
Argonne National Laboratory
P. O. Box 5207
Chicago 80, Illinois (2)

Mr. John R. Huffman
Reactor Engineering Division
Argonne National Laboratory
P. O. Box 5207
Chicago 80, Illinois (1)

Mr. Frank Kreith
Project Squid
Princeton University
Princeton, New Jersey (1)

Dr. Martin Summerfield
Project Squid
Princeton University
Princeton, New Jersey (1)

Dr. Alfred G. Lundquist
Code 429
Power Branch
Room 2714, Bldg. T-3
Office of Naval Research
Department of the Navy
Washington 25, D. C. (1)